Copper(I), silver(I), and gold(I) ethylene complexes of fluorinated and boron-methylated bis- and tris(pyridyl)borate chelators

Brandon T. Watson,^{†,1} Mukundam Vanga,^{†,1} Anurag Noonikara-Poyil,¹ Alvaro Muñoz-Castro² and H. V. Rasika Dias*,¹

- [1] Department of Chemistry and Biochemistry, The University of Texas at Arlington, Arlington, Texas 76019, USA. E-mail: dias@uta.edu
- [2] Facultad de Ingeniería, Arquitectura y Diseño, Universidad San Sebastián, Bellavista 7, Santiago, 8420524, Chile.

[†]Contributed equally to the project

Abstract

Bis- and tris-pyridyl borate ligands containing pyridyl donor arms, a methylated boron cap, and a fluorine lined coordination pocket have been prepared and utilized in coinage metal chemistry. The tris(pyridyl)borate ligand has been synthesized using a convenient boron source, [NBu₄][MeBF₃]. These N-based ligands permitted the isolation of group 11 metal-ethylene complexes [MeB(6- $(CF_3)Py)_3M(C_2H_4)$ and $[Me_2B(6-(CF_3)Py)_2]M(C_2H_4)$ (M = Cu, Ag, Au). The gold complexes display the largest coordination induced upfield shifts of the ethylene ¹³C resonance relative to that of the free ethylene in their NMR spectra while the silver complexes show the smallest shift. Solid state structures of five of these metal-ethylene complexes as well as the related free ligands were established by X-ray crystallography. Surprisingly, all three [MeB(6-(CF₃)Py)₃]M(C₂H₄) adopt the rare κ^2 coordination mode rather than the typical κ^3 coordination mode of facial capping tridentate ligands. Computational analyses indicate that κ^2 coordination mode is favored over the κ^3 -mode in these coinage metal ethylene complexes and point to the effects CF₃-substituents have on κ^2/κ^3 -energy difference. The M–C and M-N bond distances of [MeB(6-(CF₃)Py)₃]M(C₂H₄) follow the trend expected based on covalent radii of M(I) ions. The calculated ethylene-M interaction energy of κ²- $[MeB(6-(CF_3)Py)_3]M(C_2H_4)$ indicated that the gold(I) forms the strongest interaction with ethylene. A comparison to the related poly(pyrazolyl)borates is also presented.

Introduction

Since early reports by Hodgkins in 1993 on bis(pyridyl)borates (1) and Jäkle in 2012 on tris(pyridyl)borates (2),¹⁻³ there has been a growing interest in poly(pyridyl)borates,4-26 which represent a new addition to the very popular scorpionate family. 27-28 These poly(pyridyl)borates have several attractive features over the better known poly(pyrazolyl)borates as they have more thermally stable B-C linkages (compared to the relatively polar B-N linkages of the latter), foursubstitutable positions on pyridyl groups (vs. three on pyrazolyl moieties), a closer proximity of the heterocyclic ring substituent to the metal site, and are believed to be better σ-donor ligands.²³ Interestingly, despite several emerging applications, the reported poly(pyridyl)borates were limited to the parent systems based on unsubstituted pyridyl moieties $(e.g., ([Me_2B(Py)_2]^- (1), ([PhB(Py)_3]^- (2)))$ until recently. Early this year, ²⁹ our group reported the first tris(pyridyl)borate ligands with substituents at the 6-position of the pyridyl arms (see Figure 1 for labeling scheme). tert-butylphenyltris(6-trifluoromethyl-2-pyridyl)borate The ([t-BuC₆H₄B(6-(CF₃)Py)₃]⁻) serves as an excellent ligand support for the stabilization of coinage metal ethylene complexes ([t-BuC₆H₄B(6-(CF₃)Py)₃]M(C₂H₄), M = Cu(I), Ag(I), and Au(I), (3-5)).²⁹ We also reported the closely related diphenylbis(6trifluoromethyl-2-pyridyl)borate ($[Ph_2B(6-(CF_3)Py)_2]^-$), and utilized it to probe copper(I) and silver(I) carbon monoxide (*e.g.*, **6-7**) and *tert*-butyl isocyanide chemistry. Apart from these fluorinated poly(pyridyl)borates, there have been two recent studies on poly(pyridyl)borates bearing substituents on the pyridyl moieties. They include the work by Hikichi and co-workers on phenyltris(6-methyl-2-pyridyl)borate ([PhB(6-(CH₃)Py)₃]⁻) ligand and the use of its nickel(II) complexes in cyclohexane oxidation, as well as by Comito *et al.* on *iso*-propyl-, *tert*-butyl-, and mesityl- substituted phenyltris(pyridyl)borates ([PhB(6-(R)Py)₃]⁻, R = i-Pr, t-Bu, Mes), and their application in metal mediated ring-opening polymerization of lactones. Such poly(pyridyl)borate ligands with substituents at the 6-position of the pyridyl arms are quite useful as they feature larger cone-angles and are less likely to generate bis-poly(pyridyl)borate metal complexes.

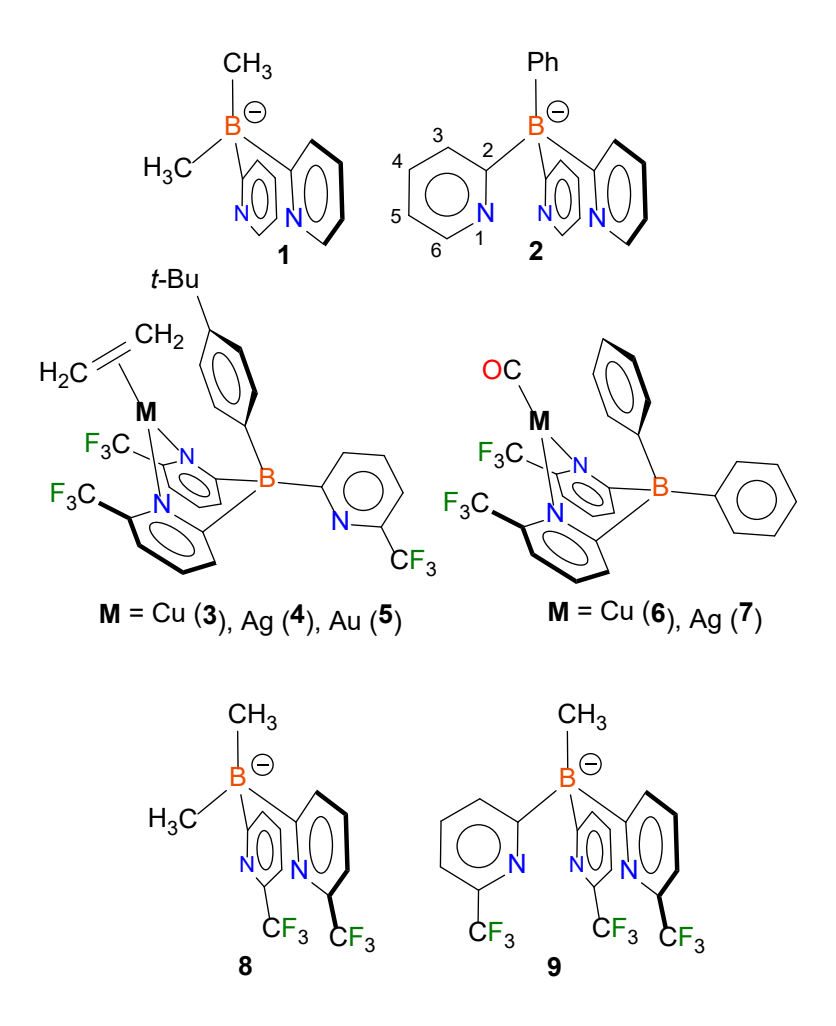


Figure 1. Bis(pyridyl)borate (**1**) and tris(pyridyl)borate (**2**) ligands, and the recently reported coinage metal complexes **3–7** of pyridyl-ring substituted, B-arylated ligand analogs, and the B-methylated ligands **8** and **9** described in this work.

Herein we report the synthesis of the first B-methylated bis- and tris-(pyridyl)borate ligands bearing substituents on the pyridyl ring 6-positions $([Me_2B(6-(CF_3)Py)_2]^-$ (8) and $[MeB(6-(CF_3)Py)_3]^-$ (9)), and their use in the stabilization of coinage metal-ethylene complexes. Isolable ethylene complexes are increasingly rare for heavier Ag and Au, 33-35 and the number of isostructural copper(I), silver(I), and gold(I) complexes of ethylene available for the study of group 11 trends are also limited in number. 36-38 That is notable considering the important roles played by coinage metals in several key applications involving ethylene. For example, copper(I) catalyzed oxychlorination of ethylene,³⁹ silver catalyzed epoxidation of ethylene to ethylene oxide, 40-41 and gold mediated 1,2difunctionalization⁴² and cyclopropanation⁴³ of ethylene are known.⁴⁴⁻⁴⁹ involvement of gold-ethylene complexes as a reagent in oxidative addition chemistry of aryl-iodides by Russel in 2018⁵⁰ and alkynylation of cyclopropenes in 2019 by Hashimi, utilizing cationic gold(I) ethylene complexes supported by 4,4'difluoro-2,2'-bipyridine and 1,10-phenanthroline as catalysts⁵¹ have been reported. Furthermore, recently, our group demonstrated the utility of polyfluorinated pyrazolate and bis(pyrazolyl)borate supported copper(I) complexes for the highly selective separation of ethylene from ethane. 52-53 Likewise, silver(I) complexes have found applications in ethylene separation.⁵⁴ Overall, coinage-metal ethylene complexes that can be isolated and investigated in detail are of significant current interest.

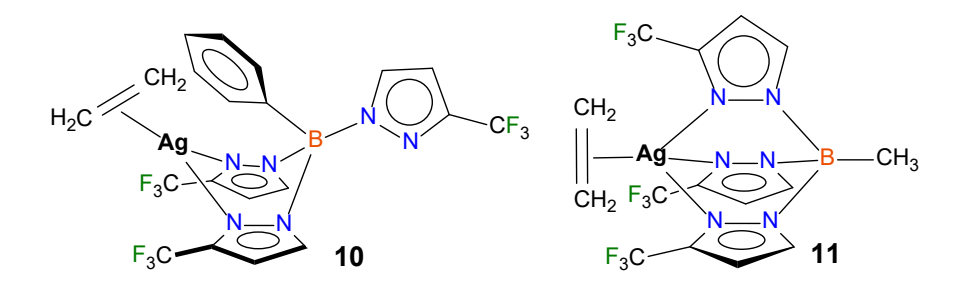


Figure 2. B-phenyl and B-methyl substituted, tris(pyrazolyl)borate silver(I) complexes of ethylene, κ^2 -[PhB(3-(CF₃)Pz)₃]Ag(C₂H₄) and κ^3 -[MeB(3-(CF₃)Pz)₃]Ag(C₂H₄) (**10**, **11**)

Coinage metal complexes **3–5** of the B-arylated tris(pyridyl)borate display the less common κ^2 coordinated mode in the solid-state with a flanking arene above metal sites (rather than the metal bound third pyridyl arm), which essentially mimics the coordination mode of diphenylbis(pyridyl)borate analogs (**6–7**) as illustrated in Figure 1. This contrasts with the common κ^3 coordination mode observed in d-block metal complexes (albeit not involving coinage metals) of B-phenylated tris(pyridyl)borate ligands based on both the pyridyl unsubstituted systems (*e.g.*, [PhB(Py)₃]⁻) and those involving non-fluorinated substituents at the pyridyl 6-position (*e.g.*, [PhB(6-(R)Py)₃]⁻ where R = Me, *i*-Pr). ³, ¹⁹⁻²⁰, ²²⁻²⁵, ³¹⁻³² Previous studies involving [PhB(3-(CF₃)Pz)₃]⁻ and [MeB(3-(CF₃)Pz)₃]⁻ with Cu(I) and Ag(I) ethylene show that the change of substituent on boron from phenyl to methyl elicits a change in the tris(pyrazolyl)borate coordination from κ^2 to κ^3 mode (*e.g.*,

Figure 2, **10** and **11**). ⁵⁵⁻⁵⁶ Thus, we are also interested in probing the effects of B-Me vs. B-aryl groups in tris(pyridyl)borate coordination modes using ligands such as **9** and to compare the outcome to the better-known tris(pyrazolyl)borates.

Results and discussion

The bis(pyridyl)borate ligand [Me₂B(6-(CF₃)Py)₂]⁻ (**8**) was prepared from the reaction of bromodimethylborane (Me₂BBr, which was freshly prepared from tetramethyltin and boron tribromide) and 6-(trifluoromethyl)-2-pyridylmagnesium chloride in dichloromethane, and isolated as a white powder (**8-H**) in 90% yield (Scheme 1). We have found that using isolated 6-(trifluoromethyl)-2-pyridylmagnesium chloride (Figure S1) greatly improves the yield of these poly(pyridyl)borate ligands compared to *in situ* generated pyridyl Grignard reagent or lithiopyridine, providing yields between 50-90% *vs.* poor yields of 10-20% obtained by *in situ* methods.^{3, 19-20, 22, 24, 29-31} It was fully characterized by several methods including multinuclear NMR spectroscopy. The two methyl groups are magnetically equivalent in the ¹H and ¹³C NMR indicating the presence of a C₂v symmetric structure in solution.

Scheme 1. Synthesis of protonated, B-methylated bis(pyridyl)borate (**8-H**) and tris(pyridyl)borate (**9-H**) ligands. The 6-(trifluoromethyl)-2-pyridylmagnesium chloride was prepared and isolated from 2-bromo-6-(trifluoromethyl)pyridine and *iso*-propylmagnesium chloride (Figure S1). Conditions (i) 2.4 eq. 6-(CF₃)PyMgCl, CH_2Cl_2 (0.1 M), -20 °C \rightarrow r.t., 48 hours, then NaHCO₃, 90% yield; (iia) M = K, 4.2 eq. 6-(CF₃)PyMgCl, THF (0.1 M), -30 °C \rightarrow r.t., 48 hours, then NaHCO₃, 20-25% yield, (iib) M = NBu₄, 4.2 eq. 6-(CF₃)PyMgCl, toluene (0.1 M), -30 °C \rightarrow r.t., 48 hours, then NaHCO₃, 51% yield.

The usual route to tris(pyridyl)borates with an aryl group on the boron center involves the treatment of the pyridyl Grignard or pyridyl lithium reagents with dihalo(aryl)boranes (ArBX₂, X = Cl or Br).^{1, 19, 23, 29, 31-32} Due to the difficult nature in preparing the boron precursor dibromo(methyl)borane (including the separation from its disproportionation byproducts, Me₂BBr, Me₃B)⁵⁷ required for the B-methylated tris(pyridyl)borate [MeB(6-(CF₃)Py)₃]⁻ (9), we searched for an alternative route involving a more user friendly boron-source. The proven utilization of air-stable RBF₃K salts (R = aryl, alkenyl) in the synthesis of triorganyl boranes (RB(R')₂) and tetraorganyl borates (RB(R')₃⁻) from R'Li or R'MgBr (R' = aryl)

motivated us to select MeBF₃K as our boron reagent of choice.⁵⁸ Initially the fluorinated methyltris(pyridyl)borate ligand [MeB(6-(CF₃)Py)₃]⁻(9) was synthesized by treating potassium methyltrifluoroborate (MeBF₃K) with 6-trifluoromethyl-2pyridylmagnesium chloride (which was obtained from iso-propylmagnesium chloride and 2-bromo-6-(trifluoromethyl)pyridine in THF, Figure S1). Although we were able to obtain the desired ligand as the protonated form (9-H) after work-up, the yields were not reproducible upon scale-up, possibly due to the instability of the 2-pyridylmagnesium chloride in THF at room temperature and the low solubility of MeBF₃K at lower temperatures. Thus, to improve the solubility of the boron reagent at lower temperatures and in inert hydrocarbon solvents, we performed tetrabutylammonium the salt metathesis with bromide to prepare tetrabutylammonium methyl trifluoroborate ([NBu₄][MeBF₃]). Utilizing this salt, we were able to prepare the protonated ligand [MeB(6-(CF₃)Py)₃]H (9-H) in gram scale in reproducible yields (Scheme 1). The 9-H was isolated as a white solid (51% yield) and fully characterized by multinuclear NMR spectroscopy and elemental analysis.

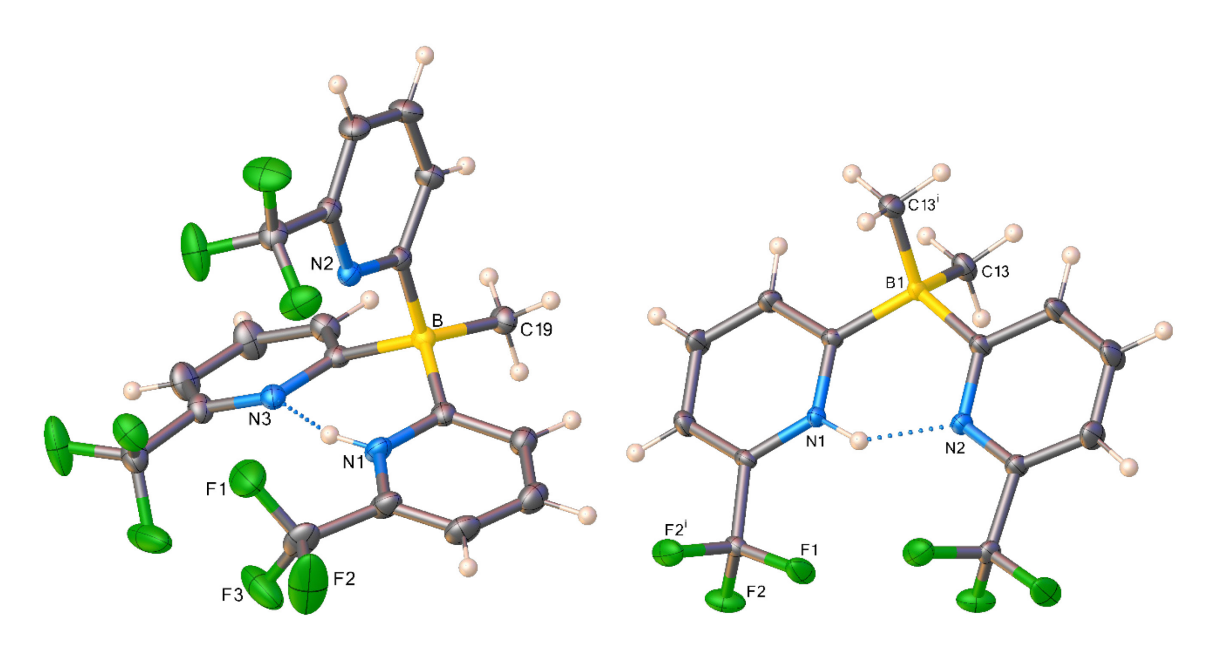


Figure 3. Molecular structures of the B-methylated tris(pyridyl)borate [MeB(6- $(CF_3)Py)_3$]H (left, **9-H**), and bis(pyridyl)borate [Me₂B(6- $(CF_3)Py)_2$]H (right, **8-H**). Thermal ellipsoid plots are shown at a 50% probability level.

We have also characterized the protonated ligands [MeB(6-(CF₃)Py)₃]H (9-H) and [Me₂B(6-(CF₃)Py)₂]H (8-H) using X-ray crystallography (Figure 3). Detailed bond distances and angles including those involving N-H moieties (Tables S1-S10) are given in the Supporting Information section. The structures of 9-H and 8-H are largely dictated by intramolecular hydrogen bonding between pyridyl rings. Examination of [MeB(6-(CF₃)Py)₃]H (9-H) reveals that two of the three pyridyl rings are nearly coplanar, with the interplanar angles between the three pyridyl rings being 103.1, 104.8, and 151.9° (where the interplanar angle is the angle between the plane of each pyridyl ring, which would all be 120° in an ideal C_{3v} structure, see

Figure S40 for details). Despite this asymmetry in the crystal structure, all three rings are magnetically equivalent in the 1 H, 13 C, and 19 F NMR, likely due to a fast intramolecular proton exchange in solution at room temperature. Additionally, the acidic NH peak was not observed for **9-H**, whereas in our previously reported protonated ligands ([t-BuC₆H₄B(6-(CF₃)Py)₃]H and [(6-(CF₃)Py)₂]H)) as well as **8-H**, the peak was observed between 19 and 20 ppm as a very broad singlet. Interestingly, [Me₂B(6-(CF₃)Py)₂]H (**8-H**) sits on a crystallographic mirror plane containing two-pyridyl arms, and features completely coplanar pyridyl rings and equivalent B-Me sites. There are two chemically similar but crystallographically distinct molecules in the asymmetric unit.

Considering the current interest in coinage metal ethylene complexes, we set out to investigate the ability of [MeB(6-(CF₃)Py)₃]⁻ (9) and [Me₂B(6-(CF₃)Py)₂]⁻ (8) to stabilize such species. For this purpose, potassium salts of the ligands 8 and 9, [Me₂B(6-(CF₃)Py)₂]K (8-K) and [MeB(6-(CF₃)Py)₃]K (9-K) were prepared by the deprotonation of the corresponding protonated ligands (8-H and 9-H) with KH and obtained in essentially quantitative yields (Scheme 2). These salts were then reacted with CuOTf, AgOTf, and AuCl under an ethylene atmosphere to prepare the corresponding copper(I), silver(I) and gold(I) ethylene complexes 12–17 (Scheme 2).

Scheme 2. Synthesis of B-methylated tris(pyridyl)borate ethylene complexes (**12–14**) supported by $[MeB(6-(CF_3)Py)_3]^-$ (**9**), and bis(pyridyl)borate ethylene complexes (**15–17**) supported by $[Me_2B(6-(CF_3)Py)_2]^-$ (**8**)

The copper(I) complexes [MeB(6-(CF₃)Py)₃]Cu(C₂H₄) (**12**) and [Me₂B(6-(CF₃)Py)₂]Cu(C₂H₄) (**15**) were stable under reduced pressure and do not lose ethylene readily, unless prolonged vacuum is applied. On the other hand, the silver(I) complexes [MeB(6-(CF₃)Py)₃]Ag(C₂H₄) (**13**) and [Me₂B(6-(CF₃)Py)₂]Ag(C₂H₄) (**16**) lose ethylene under reduced pressure. The dimethylbis(pyridyl)borate ligand supported silver(I) complex **16** displays a dynamic equilibrium with the ethylene dissociated species in CDCl₃ solution at room temperature as observed by ¹H and ¹³C NMR spectroscopy. Compounds **12**, **13**, and **15** are stable in solution at room temperature, with no observable decomposition in their NMR spectra. The gold(I)

complexes [MeB(6-(CF₃)Py)₃]Au(C₂H₄) (**14**) and [Me₂B(6-(CF₃)Py)₂]Au(C₂H₄) (**17**) are fairly stable at lower temperatures (-20 °C) both in solid state and in solution. However, both **14** and **17** gradually decompose at room temperature even in the solid state under a nitrogen atmosphere, as evident from the formation of purple solids with no observable bound ethylene (based on NMR data) within 1 hour (Figures S35-S38).

Table 1. Selected ¹H and ¹³C{¹H} NMR data (ppm) of poly(pyridyl)borate and poly(pyrazolyl)borate coinage metal ethylene complexes.

Compound	δ _H (<i>H</i> ₂ C=)	ΔδΗ	$\delta_{C}(H_{2}C=)$	Δδς	ref
					29
κ^2 -[t-BuC ₆ H ₄ B(6-(CF ₃)Py) ₃]Cu(C ₂ H ₄) (3)	3.57	-1.83	85.1	-38.0	29
κ^2 -[MeB(6-(CF ₃)Py) ₃]Cu(C ₂ H ₄) (12)	3.55	-1.85	83.3	-39.9	this work
κ^2 -[Me ₂ B(6-(CF ₃)Py) ₂]Cu(C ₂ H ₄) (15)	4.43	-0.97	82.8	-40.3	this work
κ^2 -[PhB(3-(C ₂ F ₅)Pz) ₃]Cu(C ₂ H ₄) (18)	3.70	-1.70	85.5	-37.6	36
κ^2 -[t-BuC ₆ H ₄ B(6-(CF ₃)Py) ₃]Ag(C ₂ H ₄) (4)	4.66	-0.74	103.2	-19.9	29
κ^2 -[MeB(6-(CF ₃)Py) ₃]Ag(C ₂ H ₄) (13)	4.74	-0.66	104.3	-18.8	this work
κ^2 -[Me ₂ B(6-(CF ₃)Py) ₂]Ag(C ₂ H ₄) (16)	5.42	+0.02	102.8	-20.3	this work
κ^2 -[PhB(3-(C ₂ F ₅)Pz) ₃]Ag(C ₂ H ₄) (19)	4.62	-0.78	102.0	-21.1	36
κ^2 -[t-BuC ₆ H ₄ B(6-(CF ₃)Py) ₃]Au(C ₂ H ₄) (5)	2.66	-2.74	58.7	-64.4	29
κ^2 -[MeB(6-(CF ₃)Py) ₃]Au(C ₂ H ₄) (14)	2.69	-2.71	57.6	-65.5	this work
κ^2 -[Me ₂ B(6-(CF ₃)Py) ₂]Au(C ₂ H ₄) (17)	3.41	-1.99	57.1	-66.0	this work
κ^2 -[PhB(3-(C ₂ F ₅)Pz) ₃]Au(C ₂ H ₄) (20)	2.89	-2.51	59.3	-63.8	36

 δ_{H} and δ_{C} refers to the chemical shift of the bound ethylene resonances, $\Delta\delta_{H}$ and $\Delta\delta_{C}$ refers to the change in chemical shift relative to free ethylene (5.40 (^{1}H) and 123.13 (^{13}C) in CDCl₃), where $\Delta\delta$ = δ (free ethylene resonance) - δ (ethylene resonance of the metal complex).

The key NMR spectroscopic features of the ethylene complexes are summarized in Table 1. In comparison to free ethylene, the ¹H and ¹³C NMR spectra of the copper(I) complex 12 display coordination induced upfield shifts of 1.85 ppm and 39.9 ppm for the ethylene protons and carbon resonances respectively, while the dimethylbis(pyridyl)borate supported copper(I) complex 15 displays a smaller upfield shift of 0.97 ppm in the ethylene proton signals and almost identical (40.3) ppm) shift of the ¹³C signal. The difference in the ¹H chemical shift can most likely be rationalized as an effect of the ring current of the flanking pyridyl ring (from a κ^2 -bound tris(pyridyl)borate), as the chemical shifts of 12 are quite similar to those of the previously reported *tert*-butylphenyltris(pyridyl)borate 3 and supported copper(I) complexes phenyltris(pyrazolyl)borate (e.g., [PhB(3- $(C_2F_5)Pz)_3$ Cu (C_2H_4) (18))³⁶ which both feature flanking phenyl rings and κ^2 -bound scorpionate ligands. A similar trend is also observed amongst heavier group 11 relatives, Ag and Au, between B-methyl and B-arylated systems (Table 1). example, the analogous silver(I) complex of methyltris(pyridyl)borate 13 shows an upfield chemical shift of 0.66 ppm and dimethylbis(pyridyl)borate 16 shows a downfield chemical shift of 0.02 ppm in their proton NMR, while the ¹³C peak for the silver bound ethylene groups display similar upfield chemical shifts of 18.8 and 20.3 ppm, respectively. Compared to copper and silver analogs, the gold(I)

complexes 14 and 17 display the largest upfield shifts of ethylene moiety signals in both the ¹H NMR (*i.e.*, upfield shifts of 2.71 and 1.99 ppm, respectively) and the ¹³C NMR (i.e., upfield shifts of 65.5 and 66.0 ppm, respectively) relative to those of the free ethylene (Table 1). 59-61 This trend within the coinage metal family (group 11) is also observed among the group 10 metals, nickel(II), palladium(II), and platinum(II), in which the 5d metal platinum displays the largest coordination shifts. In 2005, Forniés reported an isostructural series of group 10 ethylene complexes similar to Zeise's salt, $[NBu_4][(C_6F_5)_3M(C_2H_4)]$ (M = Ni(II), Pd(II), Pt(II)), in which the ethylene resonances were observed at δ 4.96, 5.12, and 4.33 ppm in the ¹H NMR spectra for the nickel, palladium, and platinum complexes respectively. 62-63 The ethylene resonances for the palladium and platinum complexes were reported at δ 97.6 and 78.9 ppm respectively in the ¹³C NMR, but the data on nickel were not reported, perhaps due to high reactivity.

The ¹H and ¹³C NMR spectra of the dimethylbis(pyridyl)borate silver(I) ethylene complex **16** display a rapid equilibrium with an ethylene-dissociated complex, but peaks can be unambiguously assigned to the ethylene complex and the ethylene-dissociated complex (**8-Ag**), which is indicative of a weak silver-ethylene bond (Figures S31-S33). To further probe the extent of the metal-ethylene interaction, ¹³C-¹H coupled NMR data were also collected to compare ¹J_{C-H} values

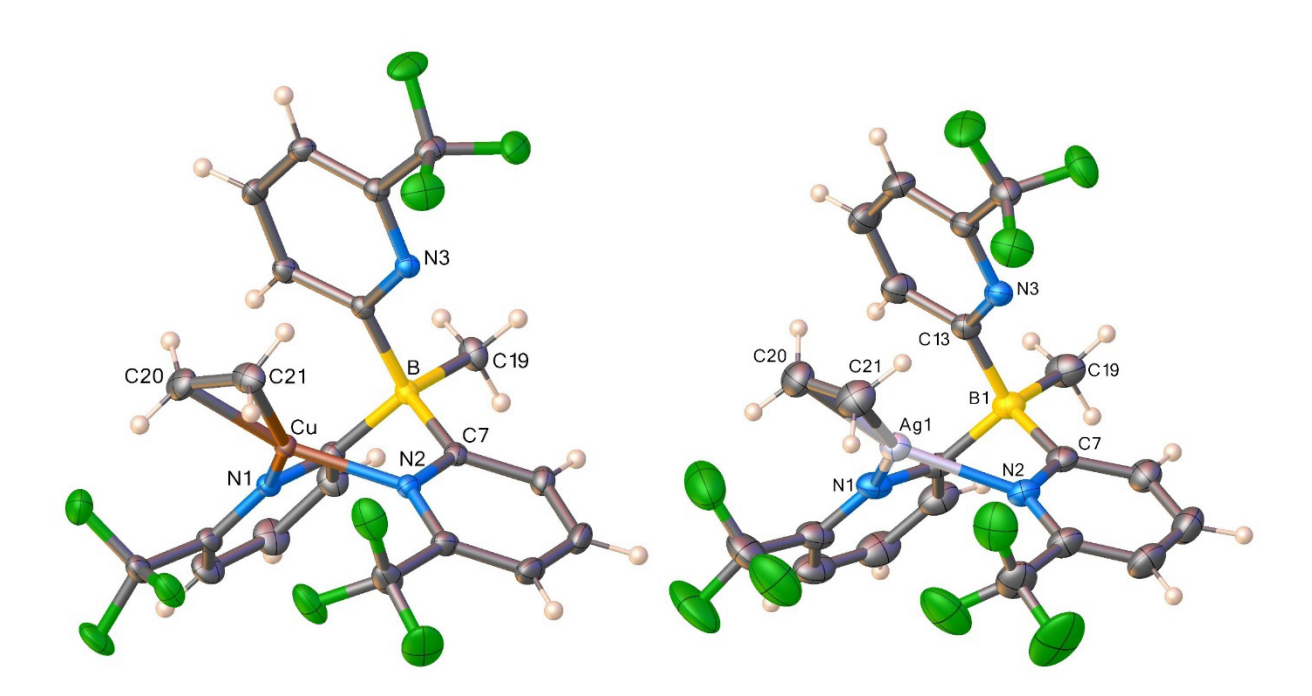
for bound ethylene (for comparison, the values for free ethylene and cyclopropane are 156 and 161 Hz respectively).^{60, 64} The bis(pyridyl)borate supported copper (**15**) and gold (**17**) complexes had coupling constants of 160.4 and 161.6 Hz respectively,⁶⁵ indicating a strong interaction while the silver complex (**16**) had a value of 153.8 Hz, closer to that of free ethylene.

Table 2. Selected bond distances (Å) and angles (deg) of coinage metal ethylene complexes of methyltris(pyridyl)borate and dimethylbis(pyridyl)borate ligands.

parameter	[MeB(6-(CF ₃)Py) ₃]	[MeB(6-(CF ₃)Py) ₃]	[MeB(6-	[Me ₂ B(6-	[Me ₂ B(6-
	Cu(C ₂ H ₄) (12)	Ag(C ₂ H ₄) (13) ^c	(CF ₃)Py) ₃]	(CF ₃)Py) ₂]	(CF ₃)Py) ₂]
			Au(C ₂ H ₄) (14)	Cu(C ₂ H ₄) (15)	Au(C ₂ H ₄) ^c (17)
C=C	1.360(2)	1.334(3)	1.409(3)	1.3670(17)	1.402(15)
		1.325(4)			1.377(16)
	2.0104(9),	2.2525(14),	2.1884(16),	2.0106(9),	2.204(8),
M-N	1.9959(9)	2.2711(14)	2.2170(15)	2.0128(9)	2.206(8)
		2.2598(13),			2.200(8),
		2.2887(13)			2.213(8)
	2.0202(12),	2.2684(19),	2.095(2),	2.0355(11),	2.102(10),
М-С	2.0240(12)	2.2720(19)	2.1040(19)	2.0382(11)	2.113(10)
		2.282(2),			2.091(10),
		2.278(2)			2.100(10)
∠NMN	93.50(4)	87.09(5)	83.42(6)	94.25(3)	85.3(3)
		84.85(4)			85.0(3)
∠CMC	39.30(6)	34.16(7)	39.21(9)	39.22(5)	38.8(4)
		33.79(9)			38.4(4)
M•••C(B) ^a	2.792	2.825	2.863	2.889	3.106
		2.746			3.07
∑ at M ^b	359.54	359.98	359.70	359.72	359.99
		359.97			359.87

M to NNCC					
plane					
distance	0.074	0.016	0.062	0.058	0.013
		0.020			0.040

^aThe M•••C(B) is the *ipso*-carbon separation between the M and flanking pyridyl or methyl groups. $^b\Sigma$ at M represents the sum of angles at M involving two nitrogen atoms bonded to M and the centroid of the ethylene carbons. ^cItalicized values represent the second molecule in the asymmetric unit.



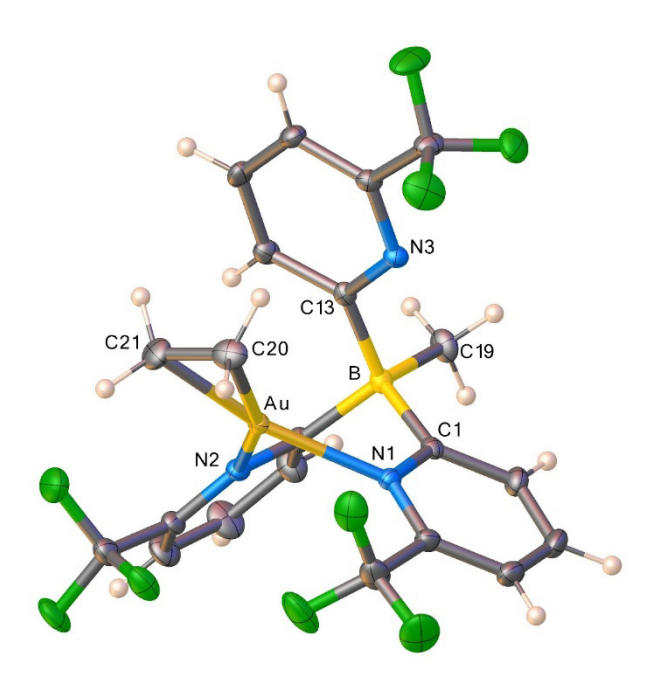


Figure 4. Molecular structures of the B-methylated tris(pyridyl)borate [MeB(6- $(CF_3)Py)_3$]Cu(C₂H₄) (top-left, **12**), [MeB(6- $(CF_3)Py)_3$]Ag(C₂H₄) (top-right, **13**), and [MeB(6- $(CF_3)Py)_3$]Au(C₂H₄) (bottom, **14**). Thermal ellipsoid plots are shown at a 50% probability level.

The analysis of the coinage metal ethylene complexes of [MeB(6-(CF₃)Py)₃]⁻ (12–14) using X-ray crystallography (Figure 4) reveals that all three are three-coordinate, trigonal planar species, featuring the κ^2 coordination mode of the tris(pyridyl)borate with two pyridyl arms coordinated, and the other twisted to be almost parallel to the metal-ethylene plane. The selected bond distances and angles are presented in Table 2. The sum of angles at the metal sites of 12–14 is essentially 360°, which is indicative of a trigonal planar coordination geometry. The observed κ^2 coordination is consistent with the relatively large upfield shifts

observed in ethylene proton signals, which were attributed to the flanking-pyridyl moieties likely present in solution. However, only one set of resonances for the pyridyl rings were observed in the ¹H, ¹³C, and ¹⁹F NMR spectra at room temperature, which suggests there is a fast interconversion of the N-coordinated and non-coordinated rings in solution. This fluxional behavior is consistent with previous findings with tris(pyrazolyl)borate coinage metal-ethylene complexes which feature κ^2 -coordination mode of the scorpionate.^{33, 35-36} This fast interconversion of pyridyl arms on the NMR time scale however, contrasts the observations involving copper(I) ethylene complex 3 (supported by B-arylated, [t-BuC₆H₄B(6-(CF₃)Py)₃]⁻), which displayed two sets of well resolved resonances in the ¹H, ¹³C, and ¹⁹F NMR for coordinated and non-coordinated pyridyl arms. This could be due to competitive phenyl/6-(CF₃)pyridyl coordination to the metal center (or preference of phenyl above metal site vs. fluorinated pyridyl moiety due to steric factors) in 3, which is not possible in the B-methylated system 12. The related tris(pyrazolyl)borate family members [MeB(3-(CF₃)Pz)₃]Cu(C₂H₄)⁵⁶ and [MeB(3- $(CF_3)Pz)_3$ Ag (C_2H_4) (11)⁵⁵ are known and they display tetrahedral metal sites and κ^3 coordination mode of the scorpionate. Thus, pyridyl and pyrazolyl ligand systems, $[MeB(6-(CF_3)Py)_3]^-$ and $[MeB(3-(CF_3)Pz)_3]^-$, adopt different modes of coordination

in their copper and silver analogs, which was not expected. The related gold(I) complex is not available for comparisons.

The molecular structures of the copper and gold ethylene complexes **15** and **17** supported by bis(pyridyl)borate [Me₂B(6-(CF₃)Py)₂]⁻ are illustrated in Figure 5. We could not obtain the crystal structure of the silver analog due to facile dissociation of ethylene. Compounds **15** and **17** display the expected κ^2 -coordination mode of the scorpionate and feature trigonal planar metal sites. Selected bond distances and angles are given in Table 2.

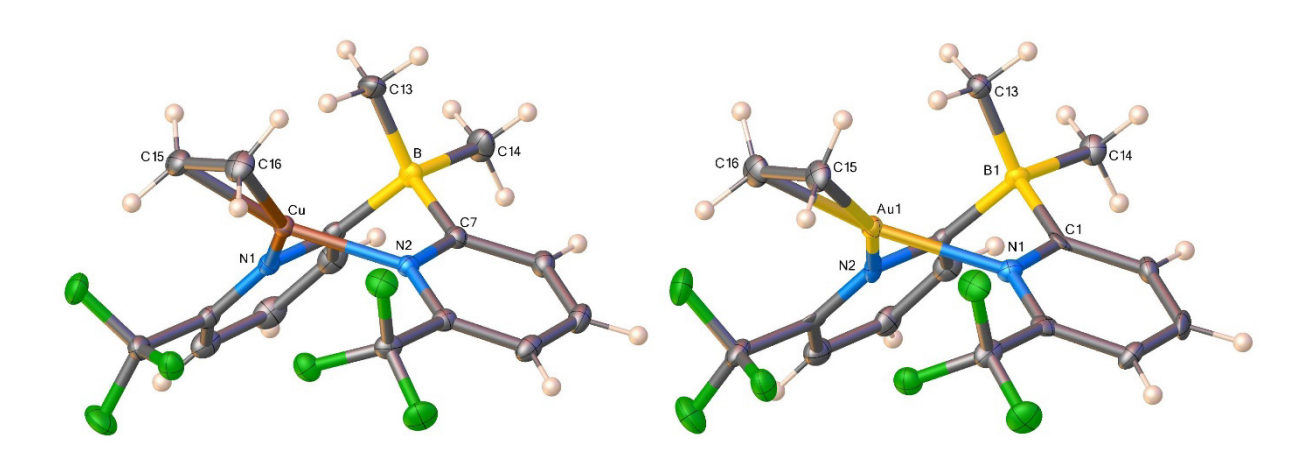


Figure 5. Molecular structures of the B-methylated bis(pyridyl)borate [Me₂B(6-(CF₃)Py)₂]Cu(C₂H₄) (left, **15**) and [Me₂B(6-(CF₃)Py)₂]Au(C₂H₄) (right, **17**). Thermal ellipsoid plots are shown at a 50% probability level.

In all five of the structurally characterized complexes the scorpionate ligand (12-14, 15 and 17) adopts the familiar B(CN)₂M boat shaped configuration involving the metal center, with the typical η^2 coordination of ethylene. Trigonal planar metal-ethylene complexes $(L_2M(C_2H_4))$ favor having the ethylene coplanar with the ligands and metal center to maximize orbital overlap and π backbonding. 66-69 The NMN and CMC planes are not exactly coplanar in the solidstate structures, where the copper(I) complexes 12 and 15 have torsion angles of 7.3° and 4.8° respectively, the silver(I) complex 16 features a torsion angle of 8.4° (average of two molecules in the asymmetric unit), and the gold complexes 14 and 17 display torsion angles of 4.6 and 3.1° (average of two molecules in the asymmetric unit), respectively. The relatively large torsion angle in the silver(I) complex 16 is perhaps indicative of the relatively weak π -backbonding capability of silver(I) compared to copper(I) and gold(I), 36, 38 as the extent of metal to olefin backdonation restricts olefin rotation from the preferred co-planar C₂MN₂ orientation.⁶⁷ This large torsion angle and weak back-donation is consistent with previous findings on isostructural coinage metal complexes. 36, 38 These torsion angles are comparably larger than the closely related poly(pyrazolyl)borate coinage metal ethylene complexes, which can be rationalized by the closer proximity of the -CF₃ group on the pyridyl ring when compared to a pyrazolyl ring. For example, the

separations between the metal center and the fluorine-bearing carbon (*e.g.* -*C*F₃ of **12–14**, **15** and **17** and -*C*F₂CF₃ of **18–20**) of the coordinated pyridyl and pyrazolyl rings are on average 3.28, 3.41, and 3.35 Å for the poly(pyridyl)borate complexes of copper(I), silver(I), and gold(I), respectively, and 3.65, 3.84, and 3.72 Å for the closely related poly(pyrazolyl)borate complexes of copper(I), silver(I), and gold(I), respectively. This close proximity of the pyridyl substituent and the steric congestion perhaps explains, at least to some degree, why κ^3 coordination was not observed with **12–14**, that have side-on bound ethylene ligands (see also the computational analysis below).

The metal to *ipso*-carbon on the boron center (either methyl or C^2 of the non-coordinated pyridyl ring) are 2.79 and 2.89 Å in the copper complexes **12** and **15**, 2.79 (av.) Å in the silver complex **13**, and 2.86, 3.09 (av.) Å in the gold complexes **14** and **17**. These separations are within the sum of van der Waals radii of M and C (for comparison, the sums of Bondi's van der Waals radii of M and C are 3.10, 3.42, and 3.36 Å for M = Cu, Ag, and Au respectively). ⁷⁰⁻⁷¹ However, these contacts do not appear significant enough to distort the coordination geometry at the metal center, as all five complexes **12–14**, **15** and **17** feature trigonal-planar metal geometries at the metal, as indicated by the sum of angles at the metal sites (~360°).

The Cu-N < Au-N < Ag-N bond lengths follow the covalent radii of M(I), as silver is bigger than both gold and copper. 72 The M—C bond lengths follow this same trend, and compare well with previously reported tris(pyrazolyl)borate and bis(pyrazolyl)methane supported coinage metal ethylene complexes. 35-36, 38, 73-75 The ethylene C=C bond lengths could be utilized to compare the degree of metalethylene σ/π -interaction in these molecules. For example, the C=C bond length in the isoleptic copper, silver, and gold-ethylene complexes 12, 13, and 14 are 1.360(2), av. 1.330(4), and 1.409(3) Å, respectively. This suggests the strongest metal-ethylene interaction in the gold adducts and the weakest in the silver complexes. In fact, the silver adduct shows essentially no change in C=C distance upon coordination to the metal, which is not surprising as these changes are typically smaller and often overshadowed by the relatively high estimated standard deviations (esds) associated with the measurement, libration effects and anisotropy of the electron density. 60,76 For comparison, the C=C bond length in free gaseous ethylene is estimated to be 1.3305(10) Å, and the corresponding X-ray data is 1.313 Å.⁷⁷⁻⁷⁸

In order to further evaluate the origin of the observed preference for κ^2 or κ^3 coordination modes within different scorpionate ligands and metal centers, computational calculations were carried out. For [MeB(6-(CF₃)Py)₃]⁻ ligands, the κ^2

coordination mode is favored by 7.5 kcal/mol over κ^3 for 12, which increases to 7.9 kcal/mol for 13, and 9.9 kcal/mol for 14, which is given by stabilization of both electrostatic and orbital interactions which overcome an increase of steric effects denoted by the destabilizing Pauli repulsion term (Table S26). The 6-(CF₃) substituents increase the energy difference between such coordination modes, by introducing steric hindrance, as compared with the calculated unsubstituted counterparts involving [MeB(Py)3] indicating a much smaller κ^2/κ^3 difference of 2.4, 1.1, and 1.2 kcal/mol for, Cu, Ag, and Au (Table S27). Replacement of the MeB group by B-phenyl substituent (PhB), as in the [PhB(6-(CF₃)Py)₃] ligand, leads to a similar but decreased preference for the κ^2 coordination mode amounting to 2.8, 4.0, and 4.8 kcal/mol, for Cu, Ag, and Au species (Table S28), respectively. These computed structures feature a more sterically demanding 6-(CF₃)Py moiety located above the metal center (instead of the Ph group), similar to the [MeB(6- $(CF_3)Py)_3 M(C_2H_4)$ species (12, 13, and 14). Interestingly, when the phenyl ring is located above the metal center, as observed in the previously characterized group of molecules, ²⁹ an energy difference between κ^2/κ^3 coordination mode isomers is increased to 19.7, 12.6, and 24.9 kcal/mol, because such disposition leads to the more sterically favorable isomer (Figure S46).

The ethylene-M interaction energy, obtained from the interplay between two fragments given by [MeB(6-(CF₃)Py)₃]M and C₂H₄, is calculated to be -44.7 kcal/mol for [MeB(6-(CF₃)Py)₃]Cu(C₂H₄) (12), which decreases to -30.0 kcal/mol in $[MeB(6-(CF_3)Py)_3]Ag(C_2H_4)$ (13), and increases to -63.3 kcal/mol in $[MeB(6-(CF_3)Py)_3]Ag(C_2H_4)$ $(CF_3)Py)_3$ Au (C_2H_4) (14). They are relatively smaller, i.e., -41.0, -19.6, and -58.7 kcal/mol, respectively, for the analogous systems with the hypothetical κ³ coordination modes, owing to an increase of steric effects accounted by the Pauli term (Table S29). In compounds **12-14**, the $M \rightarrow \pi^2$ -C₂H₄ backdonation accounts for about 60% and the M \leftarrow π^1 -C₂H₄ σ -donation is about 30% of the bonding contributions of the orbital interaction term (Table S29). The 6-(CF₃) substituents decrease the ethylene-M interaction energy slightly (Table S30) as compared to the hypothetical unsubstituted counterparts (i.e., the ethylene-metal interaction energies of Cu, Ag, and Au ethylene complexes of [MeB(Py)₃]⁻ are -46.2, -31.2, -68.2 kcal/mol, respectively). For the bis(pyridyl)borate compounds 15, 16, and 17 (Scheme 2) supported by the $[Me_2B(6-(CF_3)Py)_2]^-$, the ethylene-M interaction energy is slightly lower than those calculated for [MeB(6-(CF₃)Py)₃] species, amounting to -41.6, -26.6, and -61.9 kcal/mol (Table S31).

Interestingly, the computational analysis of κ^2 or κ^3 coordination modes of the coinage metal ethylene complexes supported by the better known pyrazolate

based scorpionates, namely [MeB(3-(CF₃)Pz)₃]⁻ and [PhB(3-(CF₃)Pz)₃]⁻, show a shift between MeB and PhB, where for the former, κ^3 coordination is favored by 1.3, 2.1, and 5.9 kcal/mol, for ethylene complexes of Cu, Ag, and Au, respectively (Table S32). In contrast, for [PhB(3-(CF₃)Pz)₃]M(C₂H₄), the κ^2 coordination mode is preferred by 13.6, 14.6, and 2.1 kcal/mol for M = Cu, Ag, and Au, respectively (Table S33), where the 3-(CF₃)Pz moiety is oriented above the metal center, in analogy to 12-14.

Conclusions

This paper describes the synthesis and coinage metal ethylene chemistry of a new "fluorine-lined" bis(pyridyl)borate and the related tris(pyridyl)borate ligand with methyl groups on the boron (vs. B-aryl systems) and CF_3 groups at the pyridyl ring 6-positions. We also demonstrate the use of an air-stable trifluoroborate [MeBF $_3$] as the boron-precursor in the ligand synthesis, avoiding the reactive and troublesome MeBBr $_2$. Furthermore, we illustrate the effects of using 6-membered pyridyl donors instead of 5-membered pyrazolyl rings in scorpionates on metal-ion coordination modes. The NMR spectroscopic data of [MeB(6-(CF_3)Py) $_3$]M(C_2H_4) and [Me $_2$ B(6-(CF_3)Py) $_2$]M(C_2H_4) (M = Cu, Ag, Au) show that the gold complexes

display the largest coordination induced upfield shifts of the ethylene ¹³C resonance (~ 66 ppm) relative to that of the free ethylene while the silver complexes show the smallest shift (~ 19 ppm). The magnitude of the metal coordination induced upfield shifts of ethylene carbon signal correlate well with the computed ethylene-M interaction energies of these metal-ethylene complexes, which point to the strongest and weakest interactions with gold(I) and silver(I), respectively. X-ray crystal structures of $[MeB(6-(CF_3)Py)_3]M(C_2H_4)$ (M = Cu, Ag, Au) and $[Me_2B(6-(CF_3)Py)_3]M(C_2H_4)$ $(CF_3)Pv_2]M(C_2H_4)$ (M = Cu, Au) show that these complexes adopt the κ^2 coordination mode of the scorpionate, which was a surprise for the former group as κ³ coordination mode is more common with such facial capping tridentate ligands. Data from the computational investigation agree with the experimental observations, which indicate that the κ^2 coordination mode is favored over the κ^3 mode in these tris(pyridyl)borate coinage metal ethylene complexes. The κ^2/κ^3 -energy difference however, is much smaller for estimated the [MeB(Py)₃]M(C₂H₄) systems which lack the CF₃-substituent, pointing to some steric influence on coordination modes. Interestingly, the coinage metal ethylene complexes of the related tris(pyrazolyl)borate show the preference for the κ^3 coordination mode. We are presently investigating the main-group and d-block metal coordination chemistry of fluorinated $[MeB(6-(CF_3)Py)_3]^-$ and $[Me_2B(6-(CF_3)Py)_2]^-$, and their utility in various applications.

Experimental Details

General information: All preparations and manipulations were carried out under an atmosphere of purified nitrogen using standard Schlenk techniques or in an MBraun drybox equipped with a -25 °C refrigerator. Dichloromethane, hexanes, toluene, and diethyl ether were dried by passing HPLC grade solvent through a Solvent Purification System (SPS, innovative technologies inc.) and stored in Straus flasks. Tetrahydrofuran was distilled from a sodium/ketyl still. Cyclohexane was distilled from sodium and degassed by 3 freeze-pump-thaw cycles. Glassware was oven dried overnight at 150 °C. NMR spectra were acquired at 25 °C, on a JEOL Eclipse 500 spectrometer and processed on MNova (¹H, 500 MHz; ¹³C, 126 MHz; ¹⁹F, 471 MHz). ¹⁹F NMR values were referenced to external CFCl₃. ¹H and ¹³C NMR spectra were referenced internally to solvent signals (CDCl₃: 7.26 ppm for ¹H NMR, 77.16 ppm for ¹³C NMR; DMSO-d₆: 2.50 ppm for ¹H NMR, 39.52 ppm for ¹³C NMR), or externally to SiMe₄ (0 ppm). ¹H, ¹³C, and ¹⁹F NMR chemical shifts are reported in ppm and coupling constants (J) are reported in Hertz (Hz). Abbreviations used for signal assignments: Py = pyridyl, s = singlet, d = doublet, t = triplet, q = quartet, q* = 1:1:1:1 quartet, m = multiplet, br s = broad singlet. NMR solvents were purchased from Cambridge Isotopes Laboratories and used as received. Ethylene gas was purchased from Matheson. Elemental analyses were performed using a Perkin-Elmer Model 2400 CHN analyzer. The compounds {(6-(CF₃)-2-Py)MgCl}₂•(THF)_x²⁹ and Me₂BBr⁷⁹ were prepared by modified literature procedures. The (CuOTf)₂•PhMe⁸⁰ was prepared according to literature procedures. All other reagents were obtained from commercial sources and used as received. Silver and gold complexes were prepared in reaction vessels protected from light using aluminum foil.

[Me₂B(6-(CF₃)Py)₂]H (8-H): Dimethylboron bromide (neat, 4.23 g, 35 mmol, 1 eq, freshly prepared and distilled) was diluted with 40 mL of dichloromethane (*ca.* 1 M solution) and cooled to 0 °C. Separately, 6-(trifluoromethyl)-2-pyridylmagnesium chloride (assumed {(6-(CF₃)-2-Py)MgCl}₂•(THF)₃, 26.4 g, 42 mmol, 1.2 eq (*i.e.*, 2.4 eq. 6-(CF₃)-2-Py)MgCl•(THF)_{1.5})) was cooled to -20 °C and dissolved in *ca.* 350 mL of dichloromethane in a 500 mL Schlenk flask. Utilizing high N₂ pressure and a bleed needle, the dimethylboron bromide solution was cannula transferred dropwise

into the Grignard solution, maintaining a temperature of -20 °C. (N.B. dimethylboron bromide is volatile (b.p. 30-31 °C), using vacuum to transfer may lower the yield). After the addition was complete, an additional 10 mL of dichloromethane can be used to rinse the dimethylboron bromide flask. The reaction was allowed to warm to room temperature and kept stirring for 48 hours. The light brown reaction mixture was added to a vigorously stirring solution of saturated sodium bicarbonate (ca. 200 mL) and left stirring for 1 hour. The organic layer was separated, and the aqueous was extracted with additional dichloromethane (3x50 mL). The organic layers were combined, washed with brine, and concentrated via rotary evaporation to yield 12 g of an orange powder which contains the 2-trifluoromethylpyridine byproduct (quenched pyridyl Grignard). This can be washed/triturated with minimal cold n-pentane to yield [Me₂B(6-(CF₃)Py)₂]H in 5.60 g yield as a pure white powder. The filtrate can be concentrated and crystallized from *n*-pentane or hexanes for additional crops, or alternatively subjected to flash column chromatography (silica gel, 10% ethyl acetate in hexanes, $R_f = 0.3$) to yield an additional 3.9 g. Single crystals can be grown from a saturated solution of dichloromethane at -20 °C or by dissolving in minimal boiling hexanes and cooling to room temperature. N.B. any future reactions using these ligands can be pooled and treated with identical work-up (NaHCO₃, crystallization or chromatographed) to reclaim the protonated ligand (**[Me₂B(6-(CF₃)Py)₂]H**) rather than discarding, in order to minimize the wastage of time and resources of repeated syntheses. Yield: 10.5 g (90%). Anal. Calc. $C_{14}H_{13}B_1F_6N_2$: C, 50.33%; H, 3.92%; N, 8.39%. Found: C, 50.17%; H, 3.91%; N, 8.27%. ¹H NMR (500 MHz, CDCl₃): δ (ppm) 19.32 (br s, 1H, NH), 8.05 (d, ³J = 9.0 Hz, 2H, Py^{3/5}), 7.86 (t, ³J = 8.0 Hz, 2H, Py⁴), 7.52 (dd, ³J = 7.7, ⁴J = 1.4 Hz, 2H, Py^{5/3}), 0.12 (s, 3H, BMe), 0.11 (s, 3H, BMe). ¹³C{¹H} NMR (126 MHz, CDCl₃): δ (ppm) 194.8 (q*, ¹ J_{C-B} = 46.9 Hz, Py²), 140.2 (q, ² J_{C-F} = 43.2 Hz, Py⁶), 137.3 (Py), 133.1 (Py), 121.2 (q, ¹ J_{C-F} = 275.2 Hz, CF₃), 116.7 (Py), 13.7 (q*, ¹ J_{C-B} = 42.1 Hz, BMe). ¹⁹F NMR (471 MHz, CDCl₃): δ (ppm) -66.76.

[MeB(6-(CF₃)Py)₃]H (9-H): To a suspension of {(6-(CF₃)-2-Py)MgCl}₂·(THF)₃ (14.39 g, 22.92 mmol, 2.1 eq) in anhydrous toluene (305 mL, *i.e.*, ~0.075 M suspension) at -30 °C was added a suspension of [NBu₄][MeBF₃] (3.55 g, 10.91 mmol, 1 eq) in anhydrous toluene (100 mL) at 0 °C. After stirring for 6 hours at 0 °C in an ice bath, the reaction mixture then slowly warmed to room temperature and continued stirring for an additional 48 hours. The reaction mixture was then poured into water (200 mL) and ethyl acetate (200 mL) mixture, 5 g of Na₂CO₃ was added, and the mixture was kept stirring for 3 hours. The layers were separated, and the aqueous layer was extracted with ethyl acetate (3 × 30 mL). The organic extracts were

combined, washed with brine, dried over Na₂SO₄, and evaporated to dryness. The resulting residue was purified through silica gel column chromatography using hexane and ethyl acetate (9:1) as eluent. The solvent was removed under reduced pressure and then the resulted solid was further recrystallized from hot hexanes to obtain the desired [MeB(6-(CF₃)Py)₃]H as a white crystalline solid. Yield: 2.6 g (51%). Anal. Calc. C₁₉H₁₃B₁F₉N₃: C, 49.06%; H, 2.82%; N, 9.03%. Found: C, 48.88%; H, 2.53%; N, 8.91%. ¹H NMR (500 MHz, CDCl₃): δ (ppm) 7.76 – 7.70 (m, 6H, Py^{3,5}), 7.45 (dd, ${}^{3}J$ = 7.3, ${}^{4}J$ = 1.6 Hz, 3H, Py⁴), 0.57 (s, 3H, BMe). 13 C{¹H} NMR (126 MHz, CDCl₃): δ (ppm) 185.9 (q*, ${}^{1}J_{C-B}$ = 51.2 Hz, Py²), 142.8 (q, ${}^{2}J_{C-F}$ = 35.8 Hz, Py⁶), 136.7 (Py), 132.1 (Py), 121.5 (q, ${}^{1}J_{C-F}$ = 274.3 Hz, Py), 116.8 (Py), 10.2 (q*, ${}^{1}J_{C-B}$ = 43.2 Hz, BMe). 19 F NMR (471 MHz, CDCl₃): δ (ppm) –67.60(s).

[Me₂B(6-(CF₃)Py)₂]K (8-K): To a suspension of KH (0.160 g, 3.90 mmol, 1.3 eq, prewashed) in 10 mL of THF at 0 °C was slowly added *via* cannula transfer a solution of [Me₂B(6-(CF₃)Py)₂]H (8-H, 1.00 g, 3.00 mmol, 1 eq) in 30 mL of THF. After complete cessation of hydrogen gas evolution, the reaction was allowed to warm temperature and kept stirring for 12 hours. Alternatively, the reaction can be brought to reflux for 1 hour. This yellow solution was filtered through a celite packed frit to remove unreacted KH. The colorless filtrate was concentrated under

reduced pressure to obtain [Me₂B(6-(CF₃)Py)₂]K as an off-white solid. The compound was further dried at 60 °C under reduced pressure overnight to remove trace solvent. Yield: 1.06 g (95%). Anal. Calc. $C_{14}H_{12}B_1F_6N_2K_1$: C, 45.18%; H, 3.25%; N, 7.53%. Found: C, 45.06%; H, 3.28%; N, 7.53%. ¹H NMR (500 MHz, DMSO-d₆): δ (ppm) 7.50 (d, 3J = 7.6 Hz, 2H, Py^{3/5}), 7.40 (t, 3J = 7.8 Hz, 2H, Py⁴), 7.15 (d, 3J = 6.9 Hz, 2H, Py^{5/3}), -0.04 (s, 6H, BMe). ${}^{13}C\{{}^{1}H\}$ NMR (126 MHz, DMSO-d₆): δ (ppm) 195.4 (q*, ${}^{1}J_{C-B}$ = 52.9 Hz, Py²), 144.4 (q, ${}^{2}J_{C-F}$ = 32.3 Hz, Py⁶), 132.2 (Py), 129.9 (Py), 123.0 (q, ${}^{1}J_{C-B}$ = 274.7 Hz, CF₃), 113.2 (Py), 14.1 (q*, ${}^{1}J_{C-B}$ = 43.3 Hz, BMe). ${}^{19}F$ NMR (471 MHz, DMSO-d₆): δ (ppm) -65.15.

[MeB(6-(CF₃)Py)₃]K (9-K): To a suspension of KH (0.26 g, 6.55 mmol, 1.5 eq) in anhydrous THF (25 mL) at 0 °C was slowly added a solution of [MeB(6-(CF₃)Py)₃]H (9-H, 2.00 g, 4.36 mmol, 1 eq) in THF (25 mL). After complete cessation of hydrogen gas evolution, the reaction mixture was allowed to warm to room temperature and then kept stirring for 12 hours. The solution was filtered through a Celite packed frit to remove unreacted KH. The solvent in the filtrate collected was removed under reduced pressure to obtain [MeB(6-(CF₃)Py)₃]K as a white solid. The compound was further dried at 90 °C for 6 hours under reduced pressure to remove

all trace solvent. Yield: 2.00 g (92%). Anal. Calc. $C_{19}H_{12}B_1F_9K_1N_3$: C, 45.35%; H, 2.40%; N, 8.35%. Found: C, 45.30%; H, 2.45%; N, 8.08%. ¹H NMR (500 MHz, DMSO-d₆): δ (ppm) 7.54 (d, 3J = 7.8 Hz, 3H, Py $^{3/5}$), 7.48 (t, 3J = 7.7 Hz, 3H, Py 4), 7.25 (d, 3J = 7.5 Hz, 3H, Py $^{5/3}$), 0.40 (s, 3H, BMe). ¹³C{¹H} NMR (126 MHz, DMSO-d₆): δ (ppm) 190.5 (q*, ${}^1J_{C-B}$ = 54.2 Hz, Py 2), 144.6 (q, ${}^2J_{C-F}$ = 32.4 Hz, Py 6), 132.5 (Py), 131.3 (Py), 122.8 (q, ${}^1J_{C-F}$ = 273.5 Hz, CF₃), 113.9 (Py), 12.0 (q*, ${}^1J_{C-B}$ = 44.4 Hz, BMe). ¹⁹F NMR (471 MHz, CDCl₃): δ (ppm) -66.15.

[MeB(6-(CF₃)Py)₃]Cu(C₂H₄) (12): To a mixture of [MeB(6-(CF₃)Py)₃]K (9-K, 150 mg, 298 µmol) and (CuOTf)₂·PhMe (85 mg, 164 µmol) in a 50 mL Schlenk flask was added anhydrous dichloromethane (20 mL) and then bubbled with ethylene. The reaction mixture was kept stirring for 3 hours then cannula filtered through a celite packed frit to remove KOTf. The solvent was then removed reduced pressure and the compound was recrystallized from ethylene saturated CH_2CI_2 /hexane mixture at -20 °C to obtain colorless X-ray quality single crystals of [MeB(6-(CF₃)Py)₃]Cu(C₂H₄). Yield: 0.141 g (85%). Anal. Calc. $C_{21}H_{16}B_1Cu_1F_9N_3$: C, 45.39%; H, 2.90%; N, 7.56%. Found: C, 45.65%; H, 3.11%; N, 7.13%. ¹H NMR (500 MHz, CDCl₃): δ (ppm) 7.74 – 7.65 (m, 6H, Py^{3,5}), 7.42 (d, 3J = 7.3 Hz, 3H, Py⁴), 3.55 (s, 4H, C_2H_4),

0.57 (s, 3H, BMe). $^{13}C\{^{1}H\}$ NMR (126 MHz, CDCl₃): δ (ppm) 187.1 (q*, $^{1}J_{C-B}$ = 54.0 Hz, Py²), 145.9 (q, $^{2}J_{C-F}$ = 31.4 Hz, Py⁶), 135.5 (Py), 132.3 (Py), 122.1 (q, $^{1}J_{C-F}$ = 273.5 Hz, CF₃), 117.1 (Py), 83.3 (C₂H₄), 11.3 (q*, $^{1}J_{C-B}$ = 44.4 Hz, BMe). ^{19}F NMR (471 MHz, CDCl₃): δ (ppm) -66.53.

 $[MeB(6-(CF_3)Py)_3]Ag(C_2H_4)$ (13): To a mixture of $[MeB(6-(CF_3)Py)_3]K$ (9-K, 150 mg, 298 µmol) and AgOTf (84 mg, 328 µmol) in a 50 mL Schlenk flask was added anhydrous dichloromethane (20 mL) and then bubbled with ethylene. The reaction mixture was kept stirring for 3 hours then cannula filtered through a celite packed frit to remove KOTf. The solvent was then removed reduced pressure and the compound was recrystallized from ethylene saturated CH₂Cl₂/hexane mixture at -20 °C to obtain colorless X-ray quality single crystals of [MeB(6-(CF₃)Py)₃]Ag(C₂H₄). Solid samples of [MeB(6-(CF₃)Py)₃]Ag(C₂H₄) lose ethylene as evidenced from its CHN analysis. Anal. Calc. C₁₉H₁₂B₁Ag₁F₉N₃: C, 39.90%; H, 2.11%; N, 7.35%. Found: C, 39.98%; H, 2.13%; N, 7.17%. Yield: 0.135 g (75%). 1 H NMR (500 MHz, CDCl₃): δ (ppm) 7.71 (d, ${}^{3}J$ = 7.9 Hz, 3H, Pv^{3/5}), 7.62 (t, ${}^{3}J$ = 7.8 Hz, 3H, Pv⁴), 7.39 (d, ${}^{3}J$ = 7.7 Hz, 3H, Py $^{5/3}$), 4.74 (s, 4H, C₂H₄), 0.55 (s, 3H, CH₃). $^{13}C\{^1H\}$ NMR (126 MHz, CDCl₃): δ (ppm) 187.6 (q*, ${}^{1}J_{C-B}$ = 52.8 Hz, Py²), 146.0 (q, ${}^{2}J_{C-F}$ = 31.7 Hz, Py⁶), 135.3 (Py), 132.1 (Py), 122.2 (q, ${}^{1}J_{C-F}$ = 273.5 Hz, CF₃), 116.3 (Py), 104.3 (C₂H₄), 11.3 (q*, ${}^{1}J_{C-B}$ = 43.2 Hz. CH₃). ¹⁹F NMR (471 MHz. CDCl₃): δ (ppm) -67.88.

[MeB(6-(CF₃)Py)₃]Au(C₂H₄) (14): Ethylene saturated dichloromethane (20 mL) at -20 °C was cannula transferred to a 50 mL Schlenk flask containing a mixture of [MeB(6-(CF₃)Py)₃]K (**9-K**, 130 mg, 0.258 mmol) and AuCl (66 mg, 0.284 mmol). The reaction mixture was slowly warmed to room temperature and kept stirred for 3 hours then cannula filtered through a celite packed frit to remove KCl. The solvent was then removed reduced pressure and the compound was recrystallized from CH₂Cl₂/hexane mixture at -20 °C to obtain colorless X-ray quality single crystals of [MeB(6-(CF₃)Py)₃]Au(C₂H₄). This complex decomposes at room temperature within 1 hour when stored under a nitrogen atmosphere. As a result, satisfactory CHN data could not be obtained. Yield: 120 mg (67%). ¹H NMR (500 MHz, CDCl₃): δ (ppm) 7.74 (d, ${}^{3}J$ = 7.6 Hz, 3H, Py^{3/5}), 7.64 (t, ${}^{3}J$ = 7.8 Hz, 3H, Py⁴), 7.44 (d, ${}^{3}J$ = 6.8 Hz, 3H, $Py^{5/3}$), 2.69 (s, 4H, C₂H₄), 0.59 (s, 3H, BMe). ¹³C{¹H} NMR (126 MHz, CDCl₃): δ (ppm) 187.7 (g*, ${}^{1}J_{C-B}$ = 52.8 Hz, Py²), 146.1 (g, ${}^{2}J_{C-F}$ = 32.7 Hz, Py⁶), 135.5 (Py), 132.6 (Py), 122.0 (q, ${}^{1}J_{C-F}$ = 273.5 Hz, CF₃), 117.2 (Py), 57.6 (C₂H₄), 11.0 (q*, ${}^{1}J_{C-B}$ = 47.0 Hz, BMe). ¹⁹F NMR (471 MHz, CDCl₃): δ (ppm) -66.87.

 $[Me_2B(6-(CF_3)Py)_2]Cu(C_2H_4)$ (15): $[Me_2B(6-(CF_3)Py)_2]K$ (8-K, 100 mg, 0.27 mmol, 1 eq) and (CuOTf)₂·PhMe (73 mg, 0.14 mmol, 0.52 eq) were combined in a 50 mL Schlenk flask and 8 mL of dichloromethane was added. Ethylene was bubbled into the solution and headspace for ca. 10 seconds every 30 minutes for 2 hours until the reaction turned colorless. Insoluble materials ((CuOTf)2·PhMe, KOTf) were removed via cannula filtration through a celite packed frit, and the solvent was removed under reduced pressure to yield a yellow powder. This was recrystallized from a concentrated dichloromethane solution at -30 °C overnight to obtain colorless X-ray quality single crystals. Yield: 0.093 g (82%). Anal. Calc. C₁₆H₁₆B₁F₆N₂Cu₁: C, 45.25%; H, 3.80%; N, 6.60%. Found: C, 44.94%; H, 3.45%; N, 6.32%. ¹H NMR (500 MHz, CDCl₃): δ (ppm) 7.95 (d, ³J = 9.0 Hz, 2H, Py^{3/5}), 7.65 (t, ³J= 8.3 Hz, 2H, Py⁴), 7.41 (d, ${}^{3}J$ = 8.7 Hz, 2H, Py^{5/3}), 4.43 (s, 4H, C₂H₄), 0.39 (s, 3H, BMe), 0.21 (s, 3H, BMe). $^{13}C\{^{1}H\}$ NMR (126 MHz, CDCl₃): δ (ppm) 192.3 (q*, $^{1}J_{C-B}$ = 47.6 Hz, Py²), 145.0 (q, ${}^{2}J_{C-F}$ = 34.2 Hz, Py⁶), 135.6 (Py), 131.5 (Py), 122.2 (q, ${}^{1}J_{C-F}$ = 274.3 Hz, CF₃), 117.2 (Py), 82.8 (C₂H₄),14.2 (q*, ${}^{1}J_{C-B}$ = 39.6 Hz, BMe), 11.1 (q*, ${}^{1}J_{C-B}$ = 46.0 Hz, BMe). ${}^{13}\text{C}-{}^{1}\text{H}$ coupled NMR (126 MHz, CDCl₃): δ (ppm) 192.3 (q*, ${}^{1}J_{C-B}$ = 48.9 Hz, Py²), 145.1 (g, ${}^{2}J_{C-F}$ = 32.8 Hz, Py⁶), 135.6 (d, ${}^{1}J_{C-H}$ = 162.8 Hz, Py), 131.5 (d, ${}^{1}J_{C-H}$ = 165.4 Hz, Py), 122.2 (q, ${}^{1}J_{C-F}$ = 274.1 Hz, CF₃), 117.2 (d, ${}^{1}J_{C-H}$ = 165.9 Hz, Py), 82.8 (t, ${}^{1}J_{C-H}$ =

160.4 Hz, C_2H_4), 14.2 (m), BMe), 11.0 (m, BMe). ¹⁹F NMR (471 MHz, CDCl₃): δ (ppm) -65.04.

 $[Me_2B(6-(CF_3)Py)_2]Ag(C_2H_4)$ (16): $[Me_2B(6-(CF_3)Py)_2]K$ (8-K, 100 mg, 0.27 mmol, 1 eq) and AgOTf (109 mg, 0.28 mmol, 0.52 eq) were combined in a 50 mL Schlenk flask and 8 mL of dichloromethane was added. Ethylene was bubbled into the solution and headspace for ca. 10 seconds every 30 minutes for 2 hours until the reaction turned colorless. Insoluble materials (AgOTf, KOTf) were removed via cannula filtration through a celite packed frit, and the solvent was removed under reduced pressure to yield a white powder. Attempts at recrystallization yielded an ethylene dissociated precipitate, in solution and solid-state this complex loses ethylene over time. Yield: 0.093 g (82%). Anal. Calc. C₁₆H₁₆B₁F₆N₂Ag₁: C, 40.98%; H, 3.44%; N, 6.25%. Found: C, 38.26%; H, 2.95%; N, 6.25%, This is a close match for ethylene dissociated C₁₄H₁₂B₁F₆N₂Ag₁: C, 38.14%; H, 2.74%; N, 6.35%. ¹H NMR (500 MHz, CDCl₃): δ (ppm) 7.93 (d, ${}^{3}J$ = 9.0 Hz, 2H, Py^{3/5}), 7.59 (t, ${}^{3}J$ = 8.0 Hz, 2H, Py⁴), 7.37 $(dd, {}^{3}J = 7.8, {}^{4}J = 1.3 Hz, 2H, Py^{5/3}), 5.42 (s, 4H, C₂H₄), 0.32 (br s, 6H, BMe₂). {}^{13}C{}^{1}H}$ NMR (126 MHz, CDCl₃): δ (ppm) 145.3 (q, ${}^{2}J_{C-F}$ = 29.6 Hz, Py⁶), 135.3 (Py), 131.3 (Py), 122.4 (q, ${}^{1}J_{C-F}$ = 273.5 Hz, CF₃), 116.2 (Py), 102.8 (C₂H₄), 12.4 (q*, ${}^{1}J_{C-B}$ = 40.8 Hz,

BMe), Py² not observed. ¹³C-¹H coupled NMR (126 MHz, CDCl₃): δ (ppm) 192.6 (q*, ${}^{1}J_{C-B}$ = 49.2 Hz, Py²), 145.1 (apparent d (theoretical q), ${}^{2}J_{C-F}$ = 34.2 Hz, Py⁶), 135.3 (d, ${}^{1}J_{C-H}$ = 162.1 Hz, Py), 131.4 (d, ${}^{1}J_{C-H}$ = 164.6 Hz, Py), 122.4 (q, ${}^{1}J_{C-F}$ = 273.0 Hz, CF₃), 116.2 (d, ${}^{1}J_{C-H}$ = 167.2 Hz, Py), 104.3 (t, ${}^{1}J_{C-H}$ = 153.8 Hz, C₂H₄), 12.4 (m, BMe). ¹⁹F NMR (471 MHz, CDCl₃): δ (ppm) -67.18.

[Me₂B(6-(CF₃)Py)₂]Au(C₂H₄) (17): [Me₂B(6-(CF₃)Py)₂]K (8-K, 100 mg, (0.27 mmol, 1 eq) and AuCl (66 mg, 0.28 mmol, 1.05 eq) were combined in a 50 mL Schlenk flask and 5 mL of cyclohexane and 1 mL of dichloromethane was added at ca. 10 °C. Ethylene was bubbled into the solution and headspace for ca. 10 seconds every 30 minutes for 1 hour until the reaction turned colorless. Insoluble materials (AuCl, KCl) were removed via cannula filtration through a celite packed frit, and the solvent was removed under reduced pressure to yield a white powder. This was recrystallized from a concentrated dichloromethane solution at -30 °C overnight to yield colorless X-ray quality single crystals. This complex decomposes within 1 hour when stored under a nitrogen atmosphere at room temperature. Consequently, satisfactory CHN analysis could not be performed. Yield: 0.131 g (88%). ¹H NMR (500 MHz, CDCl₃): δ (ppm) 8.08 (d, 3J = 8.7 Hz, 2H, Py^{3/5}), 7.86 (t, 3J = 8.3 Hz, 2H,

Py⁴), 7.52-7.48 (m, 2H, Py^{5/3}), 3.41 (s, 4H, C₂H₄), 0.38 (br s, 6H, BMe₂). ¹³C{¹H} NMR (126 MHz, CDCl₃): δ (ppm) 192.7 (q*, ${}^{1}J_{C-B}$ = 50.6 Hz, Py²), 145.5 (q, ${}^{2}J_{C-F}$ = 31.8 Hz, Py⁶), 135.8 (Py), 132.6 (Py), 122.1 (q, ${}^{1}J_{C-F}$ = 274.2 Hz, CF₃), 117.8 (Py), 57.1 (C₂H₄), 13.7 (q*, ${}^{1}J_{C-B}$ = 40.2 Hz, BMe). ¹³C-¹H coupled NMR (126 MHz, CDCl₃): δ (ppm) 192.7 (q*, ${}^{1}J_{C-B}$ = 42.2 Hz, Py²), 145.5 (q, ${}^{2}J_{C-F}$ = 31.5 Hz, Py⁶), 135.8 (d, ${}^{1}J_{C-H}$ = 164.9 Hz, Py), 132.6 (d, ${}^{1}J_{C-H}$ = 165.7 Hz, Py), 122.1 (q, ${}^{1}J_{C-F}$ = 274.3 Hz, CF₃), 117.8 (d, ${}^{1}J_{C-H}$ = 168.5 Hz, Py), 57.1 (t, ${}^{1}J_{C-H}$ = 161.6 Hz, C₂H₄), 13.5 (m, BMe. ¹⁹F NMR (471 MHz, CDCl₃): δ (ppm) -65.40.

X-ray Data Collection and Structure Determinations. A suitable crystal covered with a layer of hydrocarbon/Paratone-N oil was selected and mounted on a Cryoloop, and immediately placed in the low-temperature nitrogen stream. The X-ray intensity data of [MeB(6-(CF₃)Py)₃]H (**9-H**), [Me₂B(6-(CF₃)Py)₂]H (**8-H**), [MeB(6-(CF₃)Py)₃]Au(C₂H₄) (**13**), [MeB(6-(CF₃)Py)₃]Au(C₂H₄) (**14**), [Me₂B(6-(CF₃)Py)₂]Cu(C₂H₄) (**15**), [Me₂B(6-(CF₃)Py)₂]Au(C₂H₄) (**17**) were on a Bruker instrument with Smart ApexII detector, equipped with an Oxford Cryosystems 700 series cooler, a graphite monochromator, and a Mo K α fine-focus sealed tube (λ = 0.71073 Å). Intensity data were processed using the Bruker Apex program suite. Data were collected at 100(2) K (except the data of **13** at 150(2) K,

due to crystal cracking issues). Absorption corrections were applied by using programs in Bruker Apex3 or 4 suites. Initial atomic positions were located by SHELXT,⁸¹ and the structures of the compounds were refined by the least-squares method using SHELXL⁸² within Olex2 GUI.⁸³ All the non-hydrogen atoms were refined anisotropically. The remaining hydrogen atoms, except those noted below, were included at their calculated positions and refined as riding on the atoms to which they are joined. The hydrogen atoms on ethylene carbons of [MeB(6- $(CF_3)Py)_3$ Cu (C_2H_4) (12), [MeB(6-(CF₃)Py)₃]Ag(C₂H₄) (13), and complexes and on nitrogens of [MeB(6-(CF₃)Py)₃]H (9-H) and [Me₂B(6-(CF₃)Py)₂]H (8-H) were located in the difference map and refined freely. There are two half-molecules of [Me₂B(6-(CF₃)Py)₂]H (8-H) in the asymmetric unit, with each fragment sitting on a mirror The asymmetric unit of $[Me_2B(6-(CF_3)Py)_2]Au(C_2H_4)$ (17) contains two molecules. There were disordered hexane molecules in the asymmetric units of $[MeB(6-(CF_3)Py)_3]Cu(C_2H_4)$ (12) and $[MeB(6-(CF_3)Py)_3]Au(C_2H_4)$ (14) which could not be modeled satisfactorily, and therefore removed from the election density map using the OLEX2 solvent mask command. X-ray structural figures were generated using Olex2.83

Associated content.

Supporting Information

A file (PDF) containing additional experimental details, NMR spectra (¹H, ¹³C, ¹⁹F, ¹¹B), crystallographic data, and computational details and references.

Accession codes

CCDC files 2217123-2217124 (free ligands) and 2217125-2217129 (the metal complexes) contain the supplementary crystallographic data for molecules described above. These data can be obtained free of charge via http://www.ccdc.cam.ac.uk/conts/retrieving.html or from the Cambridge Crystallographic Data Centre (CCDC), 12 Union Road, Cambridge, CB2 1EZ, UK). Additional details are below.

Author Contributions

†Contributed equally to the project. The manuscript was written through contributions of all authors. All authors have given approval to the final version of the manuscript.

Conflict of interest

The authors declare no conflict of interest.

Acknowledgments. This material is based upon work supported by the National Science Foundation under grant number (CHE-1954456, HVRD). A.M.-C. acknowledge to FONDECYT 1221676 grant.

References

- 1. Hodgkins, T. G., The synthesis and separation of the isomeric compounds dimeric dimethyl(2-pyridyl)borane and dimethylboronium bis(2-pyridyl)dimethylborate. *Inorg. Chem.* **1993,** *32* (26), 6115-6116.
- 2. Hodgkins, T. G.; Powell, D. R., Derivatives of the Dimethylbis(2-pyridyl)borate(1–) Ion: Synthesis and Structure. *Inorg. Chem.* **1996**, *35* (7), 2140-2148.
- 3. Cui, C.; Lalancette, R. A.; Jäkle, F., The elusive tripodal tris(2-pyridyl)borate ligand: a strongly coordinating tetraarylborate. *Chem. Commun.* **2012**, *48* (55), 6930-6932.
- 4. Khaskin, E.; Zavalij, P. Y.; Vedernikov, A. N., Facile Arene C–H Bond Activation and Alkane Dehydrogenation with Anionic LPt^{II}Me₂ in Hydrocarbon–Water Systems (L = Dimethyldi(2-pyridyl)borate). *J. Am. Chem. Soc.* **2006**, *128* (40), 13054-13055.
- 5. García, F.; Hopkins, A. D.; Kowenicki, R. A.; McPartlin, M.; Silvia, J. S.; Rawson, J. M.; Rogers, M. C.; Wright, D. S., Pyridyl 'ring-flipping' in the dimers [Me₂E(2-py)]₂ (E = B, Al, Ga; 2-py = 2-pyridyl). *Chem. Commun.* **2007**, (6), 586-588.
- 6. Khaskin, E.; Zavalij, P. Y.; Vedernikov, A. N., Oxidatively Induced Methyl Transfer from Boron to Platinum in Dimethyldi(2-pyridyl)boratoplatinum Complexes. *Angew. Chem. Int. Ed.* **2007**, *46* (33), 6309-6312.

- 7. Khaskin, E.; Zavalij, P. Y.; Vedernikov, A. N., Bidirectional Transfer of Phenyl and Methyl Groups between Pt^{IV} and Boron in Platinum Dipyridylborato Complexes. *J. Am. Chem. Soc.* **2008**, *130* (31), 10088-10089.
- 8. Khaskin, E.; Lew, D. L.; Pal, S.; Vedernikov, A. N., Homogeneous catalytic transfer dehydrogenation of alkanes with a group 10 metal center. *Chem. Commun.* **2009**, (41), 6270-6272.
- 9. Conley, B. L.; Williams, T. J., Thermochemistry and Molecular Structure of a Remarkable Agostic Interaction in a Heterobifunctional Ruthenium–Boron Complex. *J. Am. Chem. Soc.* **2010**, *132* (6), 1764-1765.
- 10. Conley, B. L.; Guess, D.; Williams, T. J., A Robust, Air-Stable, Reusable Ruthenium Catalyst for Dehydrogenation of Ammonia Borane. *J. Am. Chem. Soc.* **2011**, *133* (36), 14212-14215.
- 11. Lu, Z.; Malinoski, B.; Flores, A. V.; Conley, B. L.; Guess, D.; Williams, T. J. Alcohol Dehydrogenation with a Dual Site Ruthenium, Boron Catalyst Occurs at Ruthenium *Catalysts* [Online], **2012**, p. 412-421. https://mdpires.com/d attachment/catalysts/catalysts-02-00412/article deploy/catalysts-02-00412.pdf?version=1349955945.
- 12. Pal, S.; Vedernikov, A. N., Oxidation of dimethyldi(2-pyridyl)borato $Pt^{II}Me_n$ complexes, n = 1, 0, with H_2O_2 : tandem B-to-Pt methyl group migration and formation of C–O bond. *Dalton Trans.* **2012**, *41* (26), 8116-8122.
- 13. Celaje, J. A.; Pennington-Boggio, M. K.; Flaig, R. W.; Richmond, M. G.; Williams, T. J., Synthesis and Characterization of Dimethylbis(2-pyridyl)borate Nickel(II) Complexes: Unimolecular Square-Planar to Square-Planar Rotation around Nickel(II). *Organometallics* **2014**, *33* (8), 2019-2026.

- 14. Krylova, V. A.; Djurovich, P. I.; Conley, B. L.; Haiges, R.; Whited, M. T.; Williams, T. J.; Thompson, M. E., Control of emission colour with N-heterocyclic carbene (NHC) ligands in phosphorescent three-coordinate Cu(i) complexes. *Chem. Commun.* **2014**, *50* (54), 7176-7179.
- 15. Leitl, M. J.; Krylova, V. A.; Djurovich, P. I.; Thompson, M. E.; Yersin, H., Phosphorescence versus Thermally Activated Delayed Fluorescence. Controlling Singlet–Triplet Splitting in Brightly Emitting and Sublimable Cu(I) Compounds. *J. Am. Chem. Soc.* **2014**, *136* (45), 16032-16038.
- 16. Pennington-Boggio, M. K.; Conley, B. L.; Richmond, M. G.; Williams, T. J., Synthesis, structure, and conformational dynamics of rhodium and iridium complexes of dimethylbis(2-pyridyl)borate. *Polyhedron* **2014**, *84*, 24-31.
- 17. Pal, S.; Zavalij, P. Y.; Vedernikov, A. N., Concurrent B-to-Pt Methyl Migration and B-Center Retention in Aerobic Oxidation of Methylborato Platinum(II) Complexes. *Organometallics* **2015**, *34* (20), 5183-5190.
- 18. Shi, S.; Djurovich, P. I.; Thompson, M. E., Synthesis and characterization of phosphorescent three-coordinate copper(I) complexes bearing bis(amino)cyclopropenylidene carbene (BAC). *Inorg. Chim. Acta* **2018**, *482*, 246-251.
- 19. Cui, C.; Shipman, P. R.; Lalancette, R. A.; Jäkle, F., Tris(2-pyridylborate) (Tpyb) Metal Complexes: Synthesis, Characterization, and Formation of Extrinsically Porous Materials with Large Cylindrical Channels. *Inorg. Chem.* **2013**, *52* (16), 9440-9448.
- 20. Shipman, P. O.; Cui, C.; Lupinska, P.; Lalancette, R. A.; Sheridan, J. B.; Jäkle, F., Nitroxide-Mediated Controlled Free Radical Polymerization of the Chelate

- Monomer 4-Styryl-tris(2-pyridyl)borate (StTpyb) and Supramolecular Assembly via Metal Complexation. *ACS Macro Lett.* **2013**, *2* (12), 1056-1060.
- 21. Pawar, G. M.; Lalancette, R. A.; Bonder, E. M.; Sheridan, J. B.; Jäkle, F., ROMP-Derived Pyridylborate Block Copolymers: Self-Assembly, pH-Responsive Properties, and Metal-Containing Nanostructures. *Macromolecules* **2015**, *48* (18), 6508-6515.
- 22. Jeong, S. Y.; Lalancette, R. A.; Lin, H.; Lupinska, P.; Shipman, P. O.; John, A.; Sheridan, J. B.; Jäkle, F., "Third-Generation"-Type Functional Tris(2-pyridyl)borate Ligands and Their Transition-Metal Complexes. *Inorg. Chem.* **2016**, *55* (7), 3605-3615.
- 23. Pawar, G. M.; Sheridan, J. B.; Jäkle, F., Pyridylborates as a New Type of Robust Scorpionate Ligand: From Metal Complexes to Polymeric Materials. *Eur. J. Inorg. Chem.* **2016**, *2016* (15-16), 2227-2235.
- 24. Qian, J.; Comito, R. J., A Robust Vanadium(V) Tris(2-pyridyl)borate Catalyst for Long-Lived High-Temperature Ethylene Polymerization. *Organometallics* **2021**, *40* (12), 1817-1821.
- 25. Goura, J.; McQuade, J.; Shimoyama, D.; Lalancette, R. A.; Sheridan, J. B.; Jäkle, F., Electrophilic and nucleophilic displacement reactions at the bridgehead borons of tris(pyridyl)borate scorpionate complexes. *Chem. Commun.* **2022**, *58* (7), 977-980.
- 26. Pal, S.; Zavalij, P. Y.; Vedernikov, A. N., Oxidative $C(sp^3)$ –H bond cleavage, C–C and C=C coupling at a boron center with O_2 as the oxidant mediated by platinum(II). *Chem. Commun.* **2014**, *50* (40), 5376-5378.
- 27. Trofimenko, S., Scorpionates: genesis, milestones, prognosis. *Polyhedron* **2004**, *23* (2), 197-203.

- 28. Pettinari, C., *Scorpionates II: Chelating Borate Ligands*. Imperial College Press: London, 2008.
- 29. Vanga, M.; Muñoz-Castro, A.; Dias, H. V. R., Fluorinated tris(pyridyl)borate ligand support on coinage metals. *Dalton Trans.* **2022**, *51* (4), 1308-1312.
- 30. Vanga, M.; Noonikara-Poyil, A.; Wu, J.; Dias, H. V. R., Carbonyl and Isocyanide Complexes of Copper and Silver Supported by Fluorinated Poly(pyridyl)borates. *Organometallics* **2022**, *41* (10), 1249-1260.
- 31. Fujiwara, Y.; Takayama, T.; Nakazawa, J.; Okamura, M.; Hikichi, S., Development of a novel scorpionate ligand with 6-methylpyridine and comparison of the structural and electronic properties of nickel(ii) complexes with related tris(azolyl)borates. *Dalton Trans.* **2022**, *51* (27), 10338-10342.
- 32. Qian, J.; Comito, R. J., Site-Isolated Main-Group Tris(2-pyridyl)borate Complexes by Pyridine Substitution and Their Ring-Opening Polymerization Catalysis. *Inorg. Chem.* **2022**, *61* (28), 10852-10862.
- 33. Wu, J.; Noonikara-Poyil, A.; Muñoz-Castro, A.; Dias, H. V. R., Gold(I) ethylene complexes supported by electron-rich scorpionates. *Chem. Commun.* **2021,** *57* (8), 978-981.
- 34. Dias, H. V. R.; Lovely, C. J., Carbonyl and Olefin Adducts of Coinage Metals Supported by Poly(pyrazolyl)borate and Poly(pyrazolyl)alkane Ligands and Silver Mediated Atom Transfer Reactions. *Chem. Rev.* **2008**, *108* (8), 3223-3238.
- 35. Dias, H. V. R.; Wu, J., Thermally Stable Gold(I) Ethylene Adducts: [(HB{3,5-(CF₃)₂Pz}₃)Au(CH₂=CH₂)] and [(HB{3-(CF₃),5-(Ph)Pz}₃)Au(CH₂=CH₂)]. *Angew. Chem. Int. Ed.* **2007**, *46* (41), 7814-7816.

- 36. Dias, H. V. R.; Wu, J., Structurally Similar, Thermally Stable Copper(I), Silver(I), and Gold(I) Ethylene Complexes Supported by a Fluorinated Scorpionate. *Organometallics* **2012**, *31* (4), 1511-1517.
- 37. Klimovica, K.; Kirschbaum, K.; Daugulis, O., Synthesis and Properties of "Sandwich" Diimine-Coinage Metal Ethylene Complexes. *Organometallics* **2016**, *35* (17), 2938-2943.
- 38. Mehara, J.; Watson, B. T.; Noonikara-Poyil, A.; Zacharias, A. O.; Roithová, J.; Rasika Dias, H. V., Binding Interactions in Copper, Silver and Gold π -Complexes. *Chem. Eur. J.* **2022**, *28* (13), e202103984.
- 39. Ma, H.; Wang, Y.; Qi, Y.; Rout, K. R.; Chen, D., Critical Review of Catalysis for Ethylene Oxychlorination. *ACS Catal.* **2020**, *10* (16), 9299-9319.
- 40. Tomboc, G. M.; Park, Y.; Lee, K.; Jin, K., Directing transition metal-based oxygen-functionalization catalysis. *Chem. Sci.* **2021**, *12* (26), 8967-8995.
- 41. Bukhtiyarov, V. I.; Knop-Gericke, A., Chapter 9 Ethylene Epoxidation over Silver Catalysts. In *Nanostructured Catalysts: Selective Oxidations*, The Royal Society of Chemistry: 2011; pp 214-247.
- 42. Harper, M. J.; Emmett, E. J.; Bower, J. F.; Russell, C. A., Oxidative 1,2-Difunctionalization of Ethylene via Gold-Catalyzed Oxyarylation. *J. Am. Chem. Soc.* **2017**, *139* (36), 12386-12389.
- 43. Rull, S. G.; Olmos, A.; Pérez, P. J., Gold-catalyzed ethylene cyclopropanation. *Beilstein J. Org. Chem.* **2019,** *15*, 67-71.
- 44. Lamberti, C.; Prestipino, C.; Capello, L.; Bordiga, S.; Zecchina, A.; Spoto, G.; Moreno, S. D.; Marsella, A.; Cremaschi, B.; Garilli, M.; Vidotto, S.; Leofanti, G. The CuCl₂/Al₂O₃ Catalyst Investigated in Interaction with Reagents *Int. J. Mol. Sci.* [Online], 2001, p. 230-245.

- 45. Plischke, J. K.; Benesi, A. J.; Albert Vannice, M., A ¹³C NMR study of ethylene adsorbed on reduced and oxygen-covered Ag surfaces. *J. Catal.* **1992,** *138* (1), 223-239.
- 46. Dias, H. V. R.; Wang, Z., Ethylene Oxide and Propylene Sulfide Complexes of Silver(I): Synthesis and Characterization of [HB(3,5-(CF₃)₂Pz)₃]Ag(OC₂H₄) and [HB(3,5-(CF₃)₂Pz)₃]Ag(SC₃H₆). *Inorg. Chem.* **2000**, *39* (16), 3724-3727.
- 47. Roithová, J.; Schröder, D., Gas-Phase Models for Catalysis: Alkane Activation and Olefin Epoxidation by the Triatomic Cation Ag₂O⁺. *J. Am. Chem. Soc.* **2007**, *129* (49), 15311-15318.
- 48. Böcklein, S.; Günther, S.; Reichelt, R.; Wyrwich, R.; Joas, M.; Hettstedt, C.; Ehrensperger, M.; Sicklinger, J.; Wintterlin, J., Detection and quantification of steady-state ethylene oxide formation over an Ag(111) single crystal. *J. Catal.* **2013**, *299*, 129-136.
- 49. Li, Z.; Brouwer, C.; He, C., Gold-Catalyzed Organic Transformations. *Chem. Rev.* **2008**, *108* (8), 3239-3265.
- 50. Harper, M. J.; Arthur, C. J.; Crosby, J.; Emmett, E. J.; Falconer, R. L.; Fensham-Smith, A. J.; Gates, P. J.; Leman, T.; McGrady, J. E.; Bower, J. F.; Russell, C. A., Oxidative Addition, Transmetalation, and Reductive Elimination at a 2,2'-Bipyridyl-Ligated Gold Center. *J. Am. Chem. Soc.* **2018**, *140* (12), 4440-4445.
- 51. Yang, Y.; Antoni, P.; Zimmer, M.; Sekine, K.; Mulks, F. F.; Hu, L.; Zhang, L.; Rudolph, M.; Rominger, F.; Hashmi, A. S. K., Dual Gold/Silver Catalysis Involving Alkynylgold(III) Intermediates Formed by Oxidative Addition and Silver-Catalyzed C–H Activation for the Direct Alkynylation of Cyclopropenes. *Angew. Chem. Int. Ed.* **2019**, *58* (15), 5129-5133.

- 52. Parasar, D.; Elashkar, A. H.; Yakovenko, A. A.; Jayaratna, N. B.; Edwards, B. L.; Telfer, S. G.; Dias, H. V. R.; Cowan, M. G., Overcoming Fundamental Limitations in Adsorbent Design: Alkene Adsorption by Non-porous Copper(I) Complexes. *Angew. Chem.* **2020**, *132* (47), 21187-21192.
- 53. Noonikara-Poyil, A.; Cui, H.; Yakovenko, A. A.; Stephens, P. W.; Lin, R.-B.; Wang, B.; Chen, B.; Dias, H. V. R., A Molecular Compound for Highly Selective Purification of Ethylene. *Angew. Chem.* **2021**, *133* (52), 27390-27394.
- 54. Cowan, M. G.; McDanel, W. M.; Funke, H. H.; Kohno, Y.; Gin, D. L.; Noble, R. D., High Ethene/Ethane Selectivity in 2,2'-Bipyridine-Based Silver(I) Complexes by Removal of Coordinated Solvent. *Angew. Chem.* **2015**, *127* (19), 5832-5835.
- 55. Dias, H. V. R.; Wu, J.; Wang, X.; Rangan, K., Structural Variations of Silver Ethylene Complexes Supported by Boron-Protected Fluorinated Scorpionates and the Isolation of a Ligand-Directed Silver Helix. *Inorg. Chem.* **2007**, *46* (6), 1960-1962.
- 56. Dias, H. V. R.; Wang, X.; Diyabalanage, H. V. K., Fluorinated Tris(pyrazolyl)borate Ligands without the Problematic Hydride Moiety: Isolation of Copper(I) Ethylene and Copper(I)–Tin(II) Complexes Using [MeB(3-(CF₃)Pz)₃]. *Inorg. Chem.* **2005**, *44* (21), 7322-7324.
- 57. Jaroslaw Lewkowski; Michel Vaultier, The Reaction of Tetramethylsilane with Boron Tribromide. *Main Group Met. Chem.* **2001,** *24* (1), 13-14.
- 58. Music, A.; Baumann, A. N.; Boser, F.; Müller, N.; Matz, F.; Jagau, T. C.; Didier, D., Photocatalyzed Transition-Metal-Free Oxidative Cross-Coupling Reactions of Tetraorganoborates**. *Chem. Eur. J.* **2021**, *27* (13), 4322-4326.
- 59. Kazi, A. B.; Rasika Dias, H. V.; Tekarli, S. M.; Morello, G. R.; Cundari, T. R., Coinage Metal–Ethylene Complexes Supported by Tris(pyrazolyl)borates: A Computational Study. *Organometallics* **2009**, *28* (6), 1826-1831.

- 60. Dias, H. V. R.; Wu, J., Structurally Characterized Coinage-Metal–Ethylene Complexes. *Eur. J. Inorg. Chem.* **2008**, *2008* (4), 509-522.
- 61. Muñoz-Castro, A.; Dias, H. V. R., Bonding and ¹³C-NMR properties of coinage metal tris(ethylene) and tris(norbornene) complexes: Evaluation of the role of relativistic effects from DFT calculations. *J. Comput. Chem.* **2022**, *43* (27), 1848-1855.
- 62. Forniés, J.; Martín, A.; Martín, L. F.; Menjón, B.; Tsipis, A., All-Organometallic Analogues of Zeise's Salt for the Three Group 10 Metals. *Organometallics* **2005**, *24* (14), 3539-3546.
- 63. Zeise, W. C., Von der Wirkung zwischen Platinchlorid und Alkohol, und von den dabei entstehenden neuen Substanzen. *Annalen der Physik* **1831,** *97* (4), 497-541.
- 64. Neto, Á. C.; Santos, F. P. d.; Contreras, R. H.; Rittner, R.; Tormena, C. F., Analysis of the Electronic Origin of the ¹JCH Spin–Spin Coupling Trend in 1-X-Cyclopropanes: Experimental and DFT Study. *J. Phys. Chem. A* **2008**, *112* (46), 11956-11959.
- 65. Straub, B. F.; Eisenträger, F.; Hofmann, P., A remarkably stable copper(I) ethylene complex: synthesis, spectroscopy and structure. *Chem. Comm.* **1999**, (24), 2507-2508.
- 66. Fianchini, M.; Campana, C. F.; Chilukuri, B.; Cundari, T. R.; Petricek, V.; Dias, H. V. R., Use of [SbF₆]⁻ to Isolate Cationic Copper and Silver Adducts with More than One Ethylene on the Metal Center. *Organometallics* **2013**, *32* (10), 3034-3041.
- 67. Albright, T. A.; Hoffmann, R.; Thibeault, J. C.; Thorn, D. L., Ethylene complexes. Bonding, rotational barriers, and conformational preferences. *J. Am. Chem. Soc.* **1979**, *101* (14), 3801-3812.

- 68. Rosch, N.; Hoffmann, R., Geometry of transition metal complexes with ethylene or allyl groups as the only ligands. *Inorg. Chem.* **1974,** *13* (11), 2656-2666.
- 69. Pitzer, R. M.; Schaefer, H. F., III, Conformational preferences and electronic structures of bis(η^2 -ethene)nickel(0) and tris(η^2 -ethene)nickel(0). *J. Am. Chem. Soc.* **1979**, *101* (24), 7176-7183.
- 70. Alvarez, S., A cartography of the van der Waals territories. *Dalton Trans.* **2013**, *42* (24), 8617-8636.
- 71. Bondi, A., van der Waals Volumes and Radii. *J. Phys. Chem.* **1964,** *68* (3), 441-451.
- 72. Bayler, A.; Schier, A.; Bowmaker, G. A.; Schmidbaur, H., Gold Is Smaller than Silver. Crystal Structures of [Bis(trimesitylphosphine)gold(I)] and [Bis(trimesitylphosphine)silver(I)] Tetrafluoroborate. *J. Am. Chem. Soc.* **1996**, *118* (29), 7006-7007.
- 73. Dias, H. V. R.; Wang, Z.; Jin, W., Synthesis and Chemistry of [Hydrotris(3,5-bis(trifluoromethyl)pyrazolyl)borato]silver(I) Complexes. *Inorg. Chem.* **1997,** *36* (27), 6205-6215.
- 74. Dias, H. V. R.; Lu, H.-L.; Kim, H.-J.; Polach, S. A.; Goh, T. K. H. H.; Browning, R. G.; Lovely, C. J., Copper(I) Ethylene Adducts and Aziridination Catalysts Based on Fluorinated Tris(pyrazolyl)borates $[HB(3-(CF_3),5-(R)Pz)_3]^-$ (where $R = CF_3$, C_6H_5 , H; Pz = pyrazolyl). *Organometallics* **2002**, *21* (7), 1466-1473.
- 75. Ridlen, S. G.; Wu, J.; Kulkarni, N. V.; Dias, H. V. R., Isolable Ethylene Complexes of Copper(I), Silver(I), and Gold(I) Supported by Fluorinated Scorpionates [HB{3-(CF₃),5-(CH₃)Pz}₃]⁻ and [HB{3-(CF₃),5-(Ph)Pz}₃]⁻. *Eur. J. Inorg. Chem.* **2016**, *2016* (15-16), 2573-2580.

- 76. Reisinger, A.; Trapp, N.; Knapp, C.; Himmel, D.; Breher, F.; Rüegger, H.; Krossing, I., Silver–Ethene Complexes $[Ag(\eta^2-C_2H_4)_n][Al(OR^F)_4]$ with n=1, 2, 3 (R^F=Fluorine-Substituted Group). *Chem. Eur. J.* **2009**, *15* (37), 9505-9520.
- 77. Craig, N. C.; Groner, P.; McKean, D. C., Equilibrium Structures for Butadiene and Ethylene: Compelling Evidence for Π-Electron Delocalization in Butadiene. *J. Phys. Chem. A* **2006**, *110* (23), 7461-7469.
- 78. Nes, G. J. H.; Vos, A., Single-crystal structures and electron density distributions of ethane, ethylene and acetylene. III. Single-crystal X-ray structure determination of ethylene at 85 K. *Acta Crystallogr. B: Struct. Sci. Cryst. Eng. Mater.* **1979,** *35* (11), 2593-2601.
- 79. Guindon, Y.; Yoakim, C.; Morton, H. E., Dimethylboron bromide and diphenylboron bromide: cleavage of acetals and ketals. *J. Org. Chem.* **1984**, *49* (21), 3912-3920.
- 80. Flores, D. M.; Schmidt, V. A., Intermolecular 2 + 2 Carbonyl–Olefin Photocycloadditions Enabled by Cu(I)–Norbornene MLCT. *J. Am. Chem. Soc.* **2019**, *141* (22), 8741-8745.
- 81. Sheldrick, G., SHELXT Integrated space-group and crystal-structure determination. *Acta Crystallogr. A* **2015**, *71* (1), 3-8.
- 82. Sheldrick, G., Crystal structure refinement with SHELXL. *Acta Crystallogr. C* **2015,** *71* (1), 3-8.
- 83. Dolomanov, O. V.; Bourhis, L. J.; Gildea, R. J.; Howard, J. A. K.; Puschmann, H., OLEX2: a complete structure solution, refinement and analysis program. *J. Appl. Crystallogr.* **2009**, *42* (2), 339-341.